Learning Physics-Consistent Particle Interactions

Zhichao Han ETH Zürich zhhan@ethz.ch David S. Kammer ETH Zürich dkammer@ethz.ch Olga Fink* EPFL olga.fink@epfl.ch

Abstract

Interacting particle systems play a key role in science and engineering. Access to the governing particle interaction law is fundamental for a complete understanding of such systems. However, the inherent system complexity keeps the particle interaction hidden in many cases. Machine learning methods have the potential to learn the behavior of interacting particle systems by combining experiments with data analysis methods. However, most existing algorithms focus on learning the kinetics at the particle level. Learning pairwise interaction, e.g., pairwise force or pairwise potential energy, remains an open challenge. Here, we propose an algorithm that adapts the Graph Networks framework, which contains an edge part to learn the pairwise interaction and a node part to model the dynamics at particle level. Different from existing approaches that use neural networks in both parts, we design a deterministic operator in the node part that allows to precisely infer the pairwise interactions that are consistent with underlying physical laws by only being trained to predict the particle acceleration. We test the proposed methodology on multiple datasets and demonstrate that it achieves superior performance in inferring correctly the pairwise interactions while also being consistent with the underlying physics on all the datasets. The proposed framework is scalable to larger systems and transferable to any type of particle interactions, contrary to the previously proposed purely data-driven solutions. The developed methodology can support a better understanding and discovery of the underlying particle interaction laws, and hence guide the design of materials with targeted properties.

1 Introduction

Interacting particle systems play a key role in nature and engineering as they govern planetary motion [1], mass movement processes [2] such as landslides and debris flow, bulk material packaging [3], magnetic particle transport for biomaterials [4], and many more [5, 6]. Since the macroscopic behavior of such particle systems is the result of interactions between individual particles, knowing the governing interaction law is required to better understand, model and predict the kinetic behaviour of these systems. Particle interactions are determined by a combination of various factors including contact, friction, electrostatic charge, gravity, and chemical interaction, which affect the particles at various scales. The inherent complexity of particle systems inhibits the study of the underlying interaction law. Hence, they remain largely unknown and particle systems are mostly studied in a stochastic framework or with simulations based on simplistic laws.

Recent efforts on developing machine learning (ML) methods for the discovery of particle interaction laws have shown great potential in overcoming these challenges [7–13]. These ML methods, such as the *Graph Network-based Simulators* (GNS) [14] for simulating physical processes, *Dynamics Extraction From cryo-em Map* (DEFMap) [15] for learning atomic fluctuations in proteins, the *SchNet* [16, 17] which can learn the molecular energy and the *neural relational inference model* (NRI) [18] developed for inferring heterogeneous interactions, can be applied on various types of

^{*} To whom correspondence should be addressed. Preprint. Under review.

interacting particle systems such as water particles, sand and plastically deformable particles. They allow implicit and explicit learning of the mechanical behavior of particle systems without prior assumptions and simplifications of the underlying mechanisms. A commonly applied approach is to predict directly the kinetics of the particles without explicitly modeling the interactions [16, 19–22, 14, 23]. The neural networks, then, map directly the input states to the particle acceleration, occasionally by virtue of macroscopic potential energy [14, 16, 19–21]. While these approaches give an accurate prediction of the particle system as it evolves, they do neither provide any knowledge about the fundamental laws governing the particle interactions nor are they able to extract the particle interactions precisely.

Recent work [24] proposed an explicit model for the topology of particle systems, which imposes a strong inductive bias and, hence, provides access to individual pairwise particle interactions. [24] demonstrated that their Graph Network (GN) framework predicts well the kinetics of the particles system. However, as we will show, the inferred particle interactions violate Newtonian laws of motion, such as the action-reaction property, which states that two particles exert the same but opposed force onto each other. Therefore, the extracted pairwise particle interactions do not correspond to the real underlying particle interaction *force* or *potential*, which are the fundamental properties of a physical system. The origin of these discrepancies lies in the design of the GN approach, which does not sufficiently constrain the output space, and clearly demonstrates the need for a physics-consistent Graph Neural Network framework for particle interactions.

Here, we propose a Graph Neural Network (GNN) framework that incorporates universal physical laws, specifically Newton's second law of motion, to learn the interaction potential and force of any physical particle system. The proposed algorithm, termed physics-induced graph network for particle interaction (PIG'N'PI), combines the graph neural network methodology with deterministic physics operators to guarantee physics consistency when indirectly inferring the particle interaction forces and potential energy (Fig. 1). We will show that PIG'N'PI learns the pairwise particle potential and force by only being trained to predict the particle acceleration (without providing any supervision on the particle interactions). Moreover, we will show that the inferred interactions by PIG'N'PI are physically consistent (contrary to those inferred by purely data-driven approaches). We will further demonstrate that predictions provided by PIG'N'PI are more accurate, generalize better to larger systems and are more robust to noise than those provided by purely data-driven graph network approaches. Moreover, we will demonstrate on a case study that is close to real applications that the proposed algorithm is scalable to large systems and is applicable to any type of particle interaction laws.

2 PIG'N'PI: Physics-induced Graph Network for Particle Interaction

We propose a framework that is able to infer pairwise particle forces or potential energy by simply observing particle motion in time and space. In order to provide physics-consistent results, a key requirement is that the learnt particle interactions need to satisfy Newtonian dynamics. One of the main challenges in developing such a learning algorithm is that only information on the particle position in time and space along with particle properties (*e.g.*, charge and mass) can be used for training the algorithm and no ground truth information on the interactions is available since it is very difficult to measure it in real systems.

The proposed framework comprises the following distinctive elements (Fig. 1): 1) a graph network with a strong inductive bias representing the particles, their properties and their pairwise interactions; and 2) physics-consistent kinetics imposed by a combination of a neural network for learning the edge function and a deterministic physics operator for computing the node function within the graph network architecture. In addition, the proposed framework consists of two steps: 1) training the network to predict the particle motion in time and space; and 2) extraction of the pairwise forces or the pairwise potential energy from the edge functions of the trained network.

Particle systems We consider particle systems that are moving in space and time and are subject to Newtonian dynamics without any external forces. A particle system in this research is represented by the directed graph G=(V,E), where nodes $V=\{v_1,v_2,\ldots,v_{|V|}\}$ correspond to the particles and the directed edges $E=\{e_{ij}:v_i,v_j\in V,i\neq j\}$ correspond to their interactions. The graph is fully-connected if all particles interact with each other. Each particle i, represented by a node v_i , is characterized by its time-invariant properties, such as charge q_i and mass m_i and time-dependent

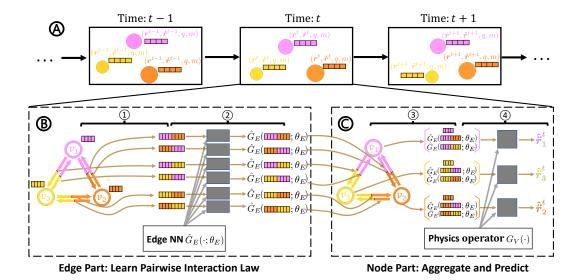


Figure 1: Framework of the proposed model to learn pairwise force or pairwise potential energy. (ⓐ) The interacting particle system contains three particles that evolve over time. At every time step, each particle is described by multiple features, which include position, velocity, charge and mass (represented by the bar). Position and velocity evolve with time whereas other properties remain constant. (ⓐ-⑤) The proposed method learns physics-consistent pairwise force or pairwise potential at every time step t. The model has two components: the edge part ⑥ and the node part ⑥. In the edge part (⑥), two nodes' vectors are concatenated as edge feature (process ①). An edge neural network $\hat{G}_E(\cdot;\theta_E)$ (θ_E represents the trainable parameters) takes the edge feature as input (process ②) and outputs a learnt vector on that edge representing the pairwise force or potential energy. In the node part (⑥), the output vectors by the edge neural network and the raw node feature are aggregated on each node (process ③). We design the deterministic node operator $G_V(\cdot)$ by incorporating physics knowledge to derive the net acceleration on nodes (process ④). By minimizing the loss on node-level accelerations, the edge neural network $\hat{G}_E(\cdot;\theta_E)$ will output pairwise force or potential energy exactly.

properties such as its position \boldsymbol{r}_i^t and its velocity $\dot{\boldsymbol{r}}_i^t$. We use $\boldsymbol{\eta}_i^t$ to denote the features of particle i at time t, $\boldsymbol{\eta}_i^t = [\boldsymbol{r}_i^t, \dot{\boldsymbol{r}}_i^t, q_i, m_i]$. We limit our evaluations to particle systems comprising homogeneous particle types. This results in particles exhibiting only one type of interaction with all its neighboring particles, leading to |E| = |V|(|V|-1). We further assume that the position \boldsymbol{r}_i^t of each particle i is observed at each time step t and that this information is available during training. Based on the position information \boldsymbol{r}_i^t , velocity $\dot{\boldsymbol{r}}_i^t$ and acceleration $\ddot{\boldsymbol{r}}_i^t$ are computed.

Proposed framework The proposed physics-induced graph network for particle interaction (PIG'N'PI) framework extends the general Graph Network framework proposed by [25], which is a generalized form of message-passing graph neural networks. The architecture of the proposed framework is illustrated in Fig. 2. We use a directed graph to represent the interacting particle system where nodes correspond to the particles and edges correspond to their interactions. The framework imposes a strong inductive bias and enables to learn the position-invariant interactions across the entire particle system network. Given the particle graph structure, the input is then defined by the node features η_i (representing particle's characteristics). The target output is the acceleration \ddot{r}_i^t of each node at time step t. The standard GNs block [25], typically, comprises two neural networks: an edge neural network $\hat{G}_E(\cdot;\theta_E)$ and a node neural network $\hat{G}_V(\cdot;\theta_V)$, where θ_E and θ_V are the trainable parameters. Here, we propose to substitute the node neural network $\hat{G}_V(\cdot;\theta_V)$ by a deterministic node operator $G_V(\cdot)$ to ensure that the learned particle interactions are consistent with the underlying physical laws. The main novelty compared to the standard GN framework is, that we impose known basic physical laws to ensure that the inferred pairwise force or potential energy corresponds to the real force or potential energy while only being trained on predicting the acceleration of the particles.

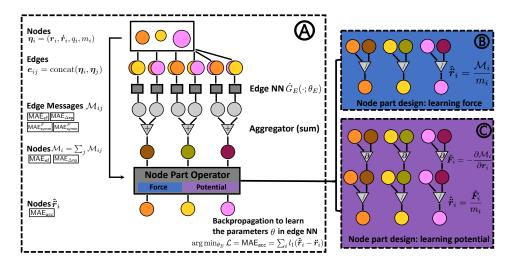


Figure 2: <u>Physics-induced graph network for particle interaction (PIG'N'PI)</u>. (A) The workflow where the edge neural network $\hat{G}_E(\cdot;\theta_E)$ takes edge features as input. The corresponding output message \mathcal{M}_{ij} is the predicted pairwise force or potential energy, depending on the physics operator (B) or (C) in the node part. Parameters θ_E in $\hat{G}_E(\cdot;\theta_E)$ are trained by minimizing the loss on particle acceleration.

It is important to emphasize that only information on particle positions is used for training the algorithm and the ground-truth information on the forces and the potential energy is not available during training. For each edge, the property vectors η_i of two nodes connected by an edge are concatenated as the edge feature vector. The edge neural network $\hat{G}_E(\cdot;\theta_E)$ outputs a message on every edge that corresponds to the pairwise force or potential energy. The output dimension is set to be the same as the spatial dimension d (two or three) if $\hat{G}_E(\cdot;\theta_E)$ is targeted to learn the pairwise force or one to learn the pairwise potential energy. Edge messages are aggregated on nodes and the node part operator computes the output corresponding to the acceleration of nodes, imposing physics-consistency on edge messages. Trained to predict the node-level acceleration, once applied to a new particle system, the GN predicts the particle motion at consecutive time steps. The pairwise forces or the pairwise potential energy can then be extracted from the edge function for each time step.

Contributions of the present work compared to precious research Here, we propose a methodology to learn the pairwise force or pairwise potential energy from the observed particle trajectories. This focus distinguishes our work from many previous works such as [26–28, 16, 29, 30] that learn the energy of the system and then derive the per-particle dynamics from the global energy. Moreover, as outlined above, our proposed approach does not have access to any ground truth information during training but rather learns to infer the force and potential energy indirectly. This is contrary to the previously proposed approaches that rely on such information [19, 23].

While our proposed framework has several similarities with two previously proposed frameworks that are also aiming to infer pairwise force and pairwise potential energy using also only the particle accelerations for training [24, 24], none of the previously proposed methods is able to infer the underlying particle interactions that are consistent with the underlying physical laws. We demonstrate in our experiments that the learnt particle interactions of the previously proposed approaches are not consistent with the underlying physical laws and do not correspond to the real forces or potential energy.

In fact, the proposed algorithm has also similarities to the Physics-informed neural networks (PINNs) [31] which aim to solve partial differential equations. Both PINNs and PIG'N'PI integrate known physical laws. While PIG'N'PI integrates Newton's second law, PINNs enforce the structure imposed by partial differential equation at a finite set of collocation points.

Table 1: The force and potential energy equations for different datasets, where F_{ij} is the force from particle j to particle i, P_{ij} is the potential incurred by particle j on particle i, r_{ij} is the Euclidean distance between particle i and particle j, n_{ij} is the unit vector pointing from particle i to particle j, q_i and m_i are the electric charge and mass of particle i. k, k, k and k are constants.

Dataset	Pairwise force (F_{ij})	Pairwise Potential (P_{ij})
Spring	$k(r_{ij}-L)m{n}_{ij}$	$\frac{1}{2}k(r_{ij}-L)^2$
Charge	$-cq_iq_jm{n}_{ij}/r_{ij}^2$	cq_iq_j/r_{ij}
Orbital	$m_i m_j oldsymbol{n}_{ij}/r_{ij}$	$m_i m_j \ln(r_{ij})$
Discnt	0 , if $r_{ij} < \Theta$ $(r_{ij} - 1)\mathbf{n}_{ij}$, otherwise	0 , if $r_{ij} < \Theta$ $0.5(r_{ij} - 1)^2$, otherwise

3 Results and discussion

3.1 Performance evaluation metrics

We evaluate the performance of the proposed PIG'N'PI framework on synthetic data generated from two- (d=2) and three- (d=3) dimensional numerical simulations. The key distinctive property of the generated datasets is the definition of the inter-particle potential energy P, which defines the inter-particle pairwise force by $\mathbf{F} = -\partial P/\partial \mathbf{r}$. The selected cases, which have also been used in prior work [24] and can be considered as a benchmark case study, cover a wide range of particle interaction features, including dependence on particle properties, e.g., mass and charge, dependence on interaction properties, e.g., stiffness, and varying degrees of smoothness (see Table 1 and SI A.10 for visualization).

The method developed by [24], which applies multilayer perceptrons (MLPs [32]) in the edge and node part, serves as the baseline for comparison. We do not change the architecture of the baseline except for changing the output dimension of its edge part MLPs when learning the pairwise force or potential energy. The output dimension is a *d*-dimensional vector for learning the pairwise force and a one-dimensional scalar for the potential energy. Besides the baseline, we compare the performance of PIG'N'PI to an alternative method proposed by [33] that is also based on GN and was specifically designed to infer pairwise forces. We denote this method as GN+ and the details are introduced in Sec. 5.4.

We split each dataset into training, validation and testing datasets and use \mathcal{T}_{train} , \mathcal{T}_{valid} and \mathcal{T}_{test} to indicate the corresponding simulation time steps for these different splits. Details regarding the dataset generation are provided in Sec. 5.5. The baseline algorithm and PIG'N'PI are trained and evaluated on the same training and testing datasets from simulations with an 8-particle system. Further, the evaluation of the generalization ability uses a 12-particle system.

It should be noted that [24] measure the quality of the learnt forces by quantifying the linear correlation between each dimension of the learnt edge message and all dimensions of the ground-truth pairwise force. This is a necessary but not sufficient condition to claim the correspondence of the learnt edge message with the pairwise interactions and to evaluate the performance of the indirect inference of the pairwise interactions. Instead, we evaluate the proposed methodology with a focus on two key aspects: 1) supervised learning performance, and 2) consistency with underlying physics. For all the evaluations, the mean absolute error on the testing dataset of various particle and interaction properties is used and is defined as follows

$$\mathsf{MAE}^{\mathrm{inter}}(\hat{\phi}, \phi) = \frac{1}{|\mathcal{T}_{\mathsf{test}}|} \frac{1}{|E|} \sum_{t \in \mathcal{T}_{\mathsf{test}}} \sum_{i,j}^{i \neq j} l_1(\hat{\phi}_{ij}^t, \phi_{ij}^t) , \qquad (1)$$

and

$$\mathsf{MAE}^{\mathrm{part}}(\hat{\phi}, \phi) = \frac{1}{|\mathcal{T}_{\mathrm{test}}|} \frac{1}{|V|} \sum_{t \in \mathcal{T}_{\mathrm{test}}} \sum_{i=1}^{|V|} l_1(\hat{\phi}_i^t, \phi_i^t) \tag{2}$$

respectively, where the superscript hat indicates the predicted values. Here, $\hat{\phi}_{ij}$ and ϕ_{ij} are the predicted and corresponding ground-truth, respectively, of a physical quantity between particle j and

particle i (e.g., pairwise force), and $\hat{\phi}_i = \sum_j \hat{\phi}_{ij}$ and $\phi_i = \sum_j \phi_{ij}$ are the aggregated prediction and the corresponding ground-truth, respectively, on particle i (e.g., net force). $l_1(x,y)$ computes the sum of absolute differences between each element in x and y, $l_1(x,y) = \sum_i |x_i - y_i|$, if x and y are vectors or the absolute difference, $l_1(x,y) = |x-y|$, if x and y are scalars. Hence, MAE^{part} measures the averaged error of the physical quantity on particles over $\mathcal{T}_{\text{test}}$, and MAE^{inter} is the averaged error of the inter-particle physical quantity over $\mathcal{T}_{\text{test}}$.

The supervised learning performance is evaluated on the prediction of the acceleration MAE_{acc}= MAE^{part}(\hat{r}, \ddot{r}). The true acceleration values serve as target values during training. The physical consistency is evaluated on two criteria. First, we evaluate the ability of the proposed framework to infer the underlying physical quantities that were not used as the target during training (*e.g.*, pairwise force), and second, we evaluate physical consistency by verifying whether Newton's action-reaction property is satisfied.

The following metrics are used to evaluate the consistency with the true pairwise interaction. For pairwise force, we use $\mathsf{MAE}_{\mathsf{ef}} = \mathsf{MAE}^{\mathsf{inter}}(\hat{\pmb{F}}, \pmb{F})$; and for potential energy case, we evaluate the increment in potential energy $\mathsf{MAE}_{\Delta\mathsf{ep}} = \mathsf{MAE}^{\mathsf{inter}}(\hat{P} - \hat{P}^0, P - P^0)$, where superscript 0 refers to the initial configuration.

For the second part of the evaluation of the physical consistency, we verify whether Newton's action-reaction property is satisfied. For that, we evaluate the symmetry in either inter-particle forces with $\mathsf{MAE}^F_{\mathsf{symm}} = \frac{1}{|\mathcal{T}_{\mathsf{lest}}|} \frac{1}{|E|} \sum_{t \in \mathcal{T}_{\mathsf{lest}}} \sum_{i,j}^{i \neq j} l_1(\hat{\pmb{F}}^t_{ij}, -\hat{\pmb{F}}^t_{ji})$ or inter-particle potential with $\mathsf{MAE}^P_{\mathsf{symm}} = \frac{1}{|\mathcal{T}_{\mathsf{lest}}|} \frac{1}{|E|} \sum_{t \in \mathcal{T}_{\mathsf{lest}}} \sum_{i,j}^{i \neq j} l_1(\hat{P}^t_{ij}, \hat{P}^t_{ji})$.

3.2 Performance evaluation between PIG'N'PI, GN+ and baseline for pairwise force

First, we analyse PIG'N'PI for application on particle systems with interactions given by pairwise forces. We start with evaluating the supervised learning performance by evaluating the prediction of the acceleration using MAE_{acc}. The results show that PIG'N'PI provides slightly better predictions than the GN+ and the baseline model for both the spring dataset (see Fig. 3D) and all other datasets (see SI A.2).

To verify the physical consistency, we first evaluate if the implicitly inferred pairwise forces are consistent with the true physical quantity. PIG'N'PI is able to infer the force field around a particle correctly, while the baseline model fails to predict the force field (see Fig. 3A for the spring dataset). A force field needs to be precise in both amplitude and direction. The error of the magnitude (see Fig. 3B) and angle (see Fig. 3C) demonstrate unambiguously the superior performance of PIG'N'PI compared to the baseline model. We quantitatively summarize the performance of the pairwise force inference with MAE_{ef}, which shows PIG'N'PI is able to infer the pairwise force correctly, while both GN+ and the baseline models fail to infer the pairwise force (2-3 orders of magnitude worse inference performance for the spring dataset (see Fig. 3D) and all other datasets (see Fig. 4A and SI A.2).

Secondly, we verify the consistency of the implicitly inferred pairwise forces with Newton's action-reaction law by evaluating the symmetry of the inter-particle forces with $\mathsf{MAE}^F_{\mathsf{symm}}$. Our results demonstrate that PIG'N'PI satisfies the symmetry property. However, GN+ and the baseline model are not able to satisfy the underlying Newton's laws for the spring dataset (see Fig. 3D) and the other datasets (see Fig. 4B and SI A.2).

Furthermore, we test the robustness of PIG'N'PI and the baseline model to learn from noisy data. We impose noise to the measured positions and then compute the noisy velocities (first-order derivative of position) and noisy accelerations (second-order derivative of position). The noisy accelerations serve then as the target values for the learning tasks of all the models. The performance of PIG'N'PI decreases with increasing noise level (see SI A.9). This is to be expected given that adding noise makes the training target (particle accelerations) less similar to the uncorrupted target that is associated with particle interactions. However, PIG'N'PI can still learn reasonably well the particle interactions despite the corrupted data. The performance of the baseline model fluctuates, however, with different noise levels significantly. This is due to the fact that the baseline model does not learn the particle interactions but rather the particle kinematics and is, therefore, more sensitive to noise.

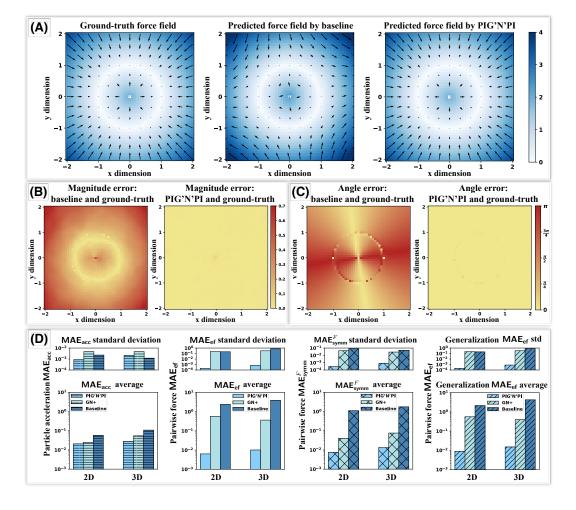


Figure 3: Case study: Quality of pairwise force prediction of PIG'N'PI and the baseline model on two-dimensional spring dataset. (A) The spring force field around a given particle. Color indicates the force amplitude. From left to right: ground-truth spring force field, predicted force field by the baseline model, predicted force field by PIG'N'PI. (B) The magnitude error between predicted force and the ground-truth force ($|\text{norm}(\hat{F}) - \text{norm}(F)|$). Left is the result of baseline model and right is the result of PIG'N'PI. (C) The angle difference between predicted force and the ground-truth force (Angle(\hat{F}, F), in radian). Left is the result of baseline model and right is the result of PIG'N'PI. (D) Comparison of the quality of PIG'N'PI, GN+ and baseline model on learning the pairwise force, where bottom is average result of five experiments and top is the corresponding standard deviation. From left to right (in logarithmic scale): acceleration error MAE_{acc}, pairwise force error MAE_{ef}, force symmetry error MAE_{symm} and pairwise force error MAE_{ef} on generalization dataset.

Finally, we note that the proposed algorithm is also able to generalize well when trained on an eight-particle system and applied to a 12-particle system for all datasets (see Fig. 3D, Fig. 4 and Table 5).

Overall, the results demonstrate that the proposed algorithm learns correctly the pairwise force (that is consistent with the underlying physics) without any direct supervision, *i.e.*, without access to the pairwise force in the first place, and that the inferred forces are consistent with the imposed underlying physical laws.

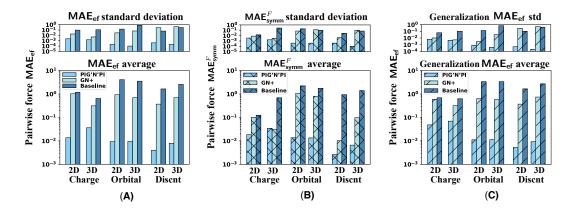


Figure 4: Quality of pairwise force prediction of PIG'N'PI, the GN+ and the baseline model. We report the average and standard deviation of different errors with five experiments, in logarithmic scale. (A) Pairwise force prediction error MAE_{ef} . (B) Pairwise force symmetry error MAE_{symm} . (C) Pairwise force error MAE_{ef} on generalization dataset.

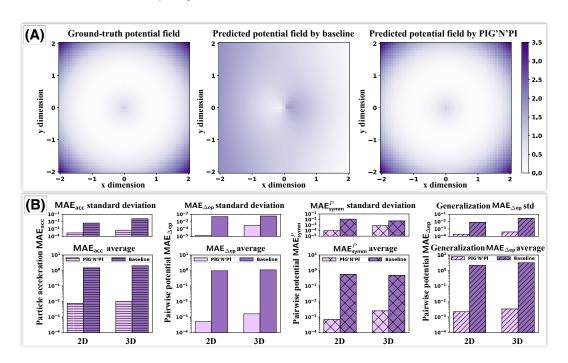
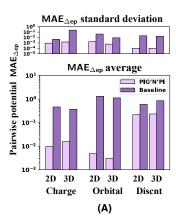
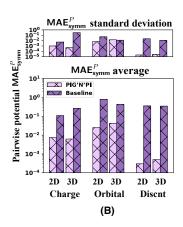


Figure 5: Case study: Quality of pairwise potential prediction of PIG'N'PI and the baseline model on Spring dataset. (A) The spring potential field around a given particle. Color indicates the potential amplitude. From left to right: ground-truth spring potential field, predicted potential field by the baseline model, predicted potential field by PIG'N'PI. (B) Comparison of the quality of PIG'N'PI and baseline model on learning the pairwise force. From left to right (in logarithmic scale): acceleration error MAE_{acc}, pairwise potential error MAE_{Δ ep}, potential symmetry error MAE $_{symm}$ and pairwise potential error MAE $_{\Delta}$ ep on generalization dataset.

3.3 Performance evaluation between PIG'N'PI and baseline for pairwise potential energy

Besides learning the pairwise force, the proposed methodology is extended to learn the pairwise potential energy (see node part design for learning potential in Sec. 2). In this case, the physics operator computes the pairwise force via partial derivative. Since GN+ was solely designed for





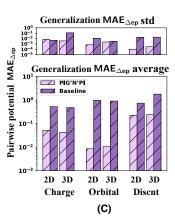


Figure 6: Quality of pairwise potential prediction of PIG'N'PI and the baseline model. We report different errors in terms of consistency with the underlying physical laws, in logarithmic scale. (A) Pairwise potential incremental error $MAE_{\Delta ep}$. (B) Pairwise potential symmetry error MAE_{symm}^{P} . (C) Pairwise potential error incremental error $MAE_{\Delta ep}$ on generalization dataset.

learning the pairwise force, it is not possible to apply it to infer the pairwise potential. Therefore, for the task of pairwise potential energy inference, we only compare PIG'N'PI with the baseline model. Our results show that PIG'N'PI performs well in the supervised learning of the acceleration (MAE_{acc}). Here again, its performance is considerably better compared to the baseline model (see Fig. 5B). Moreover, the performance is similar to that in the force-based version of the algorithm.

However, when comparing the performance of the baseline model on the supervised learning task between the potential-based version and the force-based version of the model, the performance reduces significantly in the potential-based implementation (compare to Fig. 3D). This drop of performance is potentially explained by the adjustment of the output dimension of the edge neural network in the baseline model to enable the extraction of the potential energy.

Further, our results demonstrate a superior performance of the PIG'N'PI algorithm on consistency with underlying physics. Firstly, it infers well the increment of the potential energy (see Fig. 5A). It clearly infers the increment of the potential field correctly. On the contrary, the baseline model fails to infer the potential energy. This can be quantitatively assessed with $MAE_{\Delta ep}$. The results (see Fig. 5B and 6) show that PIG'N'PI is able to infer the potential energy, while the performance of the baseline model indicates that it is not able to learn the potential energy only from observing the particles movement.

It is important to note that our algorithm cannot predict the absolute value of the potential energy; only the increment (see SI A.4). The reason is that the model is trained on the acceleration, which is computed from the derivative of the potential energy (i.e., the force). Hence, the model only constrains the derivative, and the constant of integration remains unknown. This limitation can be overcome by one of the two following options: either the potential energy is constrained by a spatial boundary condition or by an initial condition. In the former, we can impose a known value for a given value of r_{ij} , e.g., we could use the assumption that the potential energy for a charge interaction approaches zero with increasing particle distance. The alternative (but less likely) approach consists in knowing the potential energy at a given time, e.g., at the beginning of the observation and add the inferred increment to the known initial value. Nevertheless, knowing the absolute value of the potential energy is, in fact, not crucial as only its derivative determines the dynamics of a particle system. This is also confirmed in our experiments by the accurate prediction of the acceleration (see MAE $_{\rm acc}$).

Secondly, similar to the pairwise force prediction, PIG'N'PI also provides a superior performance on satisfying Newton's action-reaction property, while again, the baseline model fails to satisfy the underlying Newton's law. The performance is quantified by the symmetry of the inter-particle potential energies (MAE $_{\text{symm}}^{P}$). (Fig. 5B, Fig. 6 and Table 4).

Finally, we test the generalization ability of the learning algorithms in a similar way as in the pairwise force case study. We apply the models trained on an eight-particles system to a new particle system comprising 12 particles. The results (see SI A.3) show that PIG'N'PI predicts well the pairwise force and potential energy, and outperforms considerably the baseline model (see Fig. 5B and Fig. 6). This demonstrates that the PIG'N'PI model provides a general model for learning particle interactions.

3.4 Case study under more realistic conditions: learning pairwise interactions for a LJ-argon system

To evaluate the performance of the proposed framework on a more realistic system with a larger particle interaction system (to evaluate the scalability), we apply PIG'N'PI on a large Lennard-Jones system.

We adopt the dataset introduced in [34]. This dataset simulates the movements of liquid argon atoms governed by the Lennard-Jones (LJ) potential. The LJ potential, which is given by $V(r) = 4\epsilon\{(\sigma/r)^12 - (\sigma/r)^6\}$, is an extensively used governing law for two non-bonding atoms [35]. The simulation contains 258 particles in a cubic box whose length is 27.27 Å. The simulation is run at 100 K with periodic boundary conditions. The potential well depth ϵ is set to 0.238 kilocalorie / mole, the van der Waals radius σ is set to 3.4 Å, and the interaction cutoff radius for the argon atoms is set to 3σ . The mass of argon atom is 39.9 dalton. The dataset is run for 10 independent simulations. Each simulation contains 1000 time steps with randomly initialized positions and velocities. The position, velocity and acceleration of all particles are recorded at each time step.

Fig. 7 summarizes the learning pipeline. Contrary to the previous case study where for a small number of particles, a fully connected graph is considered, in this case study, we construct the graph of neighboring particles at every time step (Fig. 7). We connect the particles within the defined interaction cutoff radius while taking the periodic boundary conditions into consideration. Particles in the LJ-argon system are characterized by their position, velocity and mass. The charge is not part of the particle properties, which is different from the particle systems considered in the previous case study (Sec. 3.2 and Sec. 3.3). Moreover, we compute the position difference under the periodic boundary condition and use it as an edge feature. This edge feature is required because the distance between two particles in this simulation does not correspond to the Euclidean distance in the real world due to the periodic boundary conditions. The node features and the edge features are then concatenated and are used as the input to the edge part of PIG'N'PI (Fig. 7C) or the baseline model. Similarly to the previous case study, the learning target is the accelerations of the particles. The pairwise force and pairwise potential energy are then inferred from the intermediate output of the edge part.

We evaluate the performance of PIG'N'PI on inferring pairwise interactions of the LJ-argon particle system with the same performance metrics as in the previous case study. The results are reported in Fig. 8 and Table 7. Because the particles in this dataset have the same mass, we also test a variant of GN+ such that we assign all nodes with a unique learnable scalar. We denote this variant as GN+_{uni}. The results confirm the very good performance of PIG'N'PI as observed in the previous case study. Generally, GN+_{uni} outperforms the GN+, but PIG'N'PI still surpasses GN+_{uni} and the baseline. On the one hand PIG'N'PI performs better than the baseline, GN+, and GN+_{uni} on the supervised prediction task of predicting the acceleration (achieving less than half of the MAE_{acc} compared to the baseline and the GN+_{uni} (Fig. 8A)). On the other hand, PIG'N'PI is also able to infer the learn pairwise force correctly. Again, the baseline model is not able to infer the pairwise force (PIG'N'PI outperforms the baseline by more than two orders of the magnitude on the MAE_{ef}). Moreover, the particle interactions inferred by PIG'N'PI are consistent with Newton's action-reaction law (MAE^F_{symm}). The bad performance of the baseline model indicates that the learnt interactions do not satisfy the Newton's law.

To summarize, similar to the cases discussed in Sec. 3.2, PIG'N'PI learns the pairwise force well without any direct supervision for this complex and large system.

Besides, we test PIG'N'PI to learn the pairwise potential energy for this LJ system. Results are reported in Fig. 9 and Table 8. We first examine the MAE_{acc} that is the learning target. The MAE_{acc} of PIG'N'PI is similar to that in the force-based version of the algorithm. PIG'N'PI performs significantly better than the baseline model with more than 2 orders of magnitude (Fig. 9A). And, similar to the cases in Sec. 3.3, we again observe the performance drop of the baseline model in this

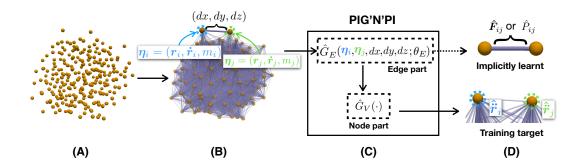


Figure 7: Pipeline of PIG'N'PI to learn pairwise force or potential for the LJ-argon particle data. Solid-line arrows indicate the data processing path from the input to the output. The dash-line arrow depicts the intermediate output of every edge corresponding to the inferred pairwise force or potential energy. (A) Positions of 258 particles at a random time step. (B) Representation of the constructed graph. Node features comprise position, velocity and mass. Edge features comprise the relative position difference under periodic boundary conditions. (C) PIG'N'PI. Edge part takes the concatenation of two nodes' features and the edge feature as input and infers the pairwise force or potential. Node part aggregates the output on every edge and predicts the acceleration. (D) The inferred pairwise force or potential by edge part and the acceleration by node part.

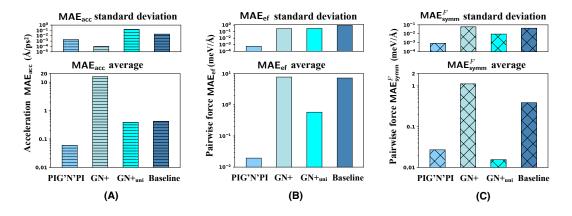
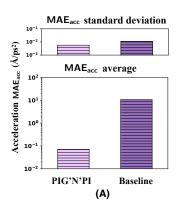
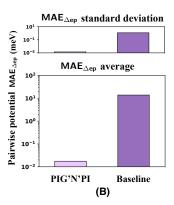


Figure 8: **Performance of the algorithms on pairwise force predictions on the LJ-argon system.** We report the MAE on the acceleration prediction, which is the target for the learning task (A), the MAE on the pairwise force inference (indirect inference task) $\mathsf{MAE}_{\mathsf{ef}}$ (B) and the consistency with Newton's action-reaction property: the MAE on pairwise force symmetry $\mathsf{MAE}_{\mathsf{symm}}^F$ (C). The average (plots at the bottom) on logarithmic scale and standard deviation (plots in the top row) are computed from five experiments.

potential-based version with the force-based version. Then, we evaluate the $MAE_{\Delta ep}$ and MAE_{ef} that are the two metrics for measuring the quality of the learnt pairwise potential energy. Results show that PIG'N'PI provides again superior performance on inferring the increment of the potential energy $MAE_{\Delta ep}$ (Fig. 9B). The bad performance of the baseline model clearly shows that it is not able to infer the potential energy correctly. Finally, we check Newton's action-reaction property in the potential energy by MAE_{symm}^P . Here again, the potential energy inferred by PIG'N'PI follows Newton's laws while the baseline model fails to infer the underlying interaction laws correctly (Fig. 9D). All evaluations demonstrate that the predicted pairwise potential energy by PIG'N'PI is consistent with the LJ potential used in the simulation, even though PIG'N'PI does not access the ground truth information.

The results on this case study demonstrate the scalability of PIG'N'PI to larger systems and the applicability to more realistic case studies. Moreover, the results confirm the results obtained in the





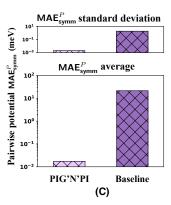


Figure 9: Quality of pairwise potential prediction on the LJ-argon data. We report different errors in *logarithmic* scale. The average and standard deviation are computed from five experiments. (A) Acceleration prediction error MAE_{acc}. (B) Pairwise potential incremental error MAE_{Δ ep}. (C) Pairwise potential symmetry error MAE $_{\text{symm}}^{P}$.

previous case study that PIG'N'PI is able to infer the underlying interaction laws correctly. While the other baseline methods are able to precisely predict the particle dynamics, they fail to infer the underlying pairwise interaction laws correctly.

3.5 Comparison of PIG'N'PI to alternative hyperparameter choices and an alternative regularized architecture

We compare the performance of the proposed approach first to alternative hyperparameter choices, in particular to different activation functions, and, second, to an alternative way of imposing physical consistency in the network architecture.

First, we evaluate different choices of activation functions following the observations made in previous studies [23, 36, 20] that confirmed their significant influence on the performance of MLPs in approximating physical quantities. The performance of PIG'N'PI with different activation functions is reported in SI A.6. The results demonstrate that PIG'N'PI with SiLU activation function (which was in fact used in all case studies) performs consistently best on most test datasets compared to PIG'N'PI with other commonly used activation functions, such as ReLU or LeakyReLU. Based on this observation, the performance of the baseline with the SiLU activation function was evaluated (SI A.2). The results show that the SiLU activation improves the learning performance of the baseline model to some degree (when only evaluating the prediction performance MAE_{acc}). However, it still performs consistently worse than PIG'N'PI and, more importantly, the consistency with underlying physics in terms of the inferred force (or potential) and interaction symmetry worsens even considerably.

Second, we compare the performance of PIG'N'PI to an alternative way of imposing physical consistency: we add a regularization into the baseline model to enforce the symmetry property onto the output messages of the edge function. The goal of imposing the symmetry regularization term is to ensure that the model satisfies the action-reaction physical consistency requirement. It is expected that by satisfying this symmetry constraint, the model performance on learning physics-consistent pairwise forces and potential energy can be improved. We add a symmetry regularization term on the learnt pairwise corresponding messages to enforce the action-reaction property. The details on this regularization term can be found in Sec. 5.3.

While the performance is improved compared to the baseline model without any regularization, the results demonstrate that PIG'N'PI still performs considerably better on inferring physical meaningful quantities for the pairwise force and potential energy than the symmetry-regularized baseline model (see SI A.8 for detailed results and SI A.5 for the evaluation on the LJ-argon system).

4 Conclusions

In this paper, we propose the Physics-induced Graph Network for Particle Interaction algorithm to learn particle interactions that are consistent with the underlying physical laws. The main novelty of the proposed algorithm is in the design of the physics operator in the node part. The designed physics operator on nodes guides the edge neural network to learn the pairwise force or pairwise potential energy exactly. This design also reduces the model complexity for this machine learning algorithm by reducing the number of tunable parameters.

While our method shows a similar performance on the supervised learning task of predicting accelerations compared to the other baseline models (purely data-driven graph networks), it is also able to infer the particle interactions correctly that follow the underlying physical laws. However, while the baseline models are able to be applied as simulators, they fail to infer physically consistent particle interactions that satisfy Newton's laws. Moreover, the proposed PIG'N'PI also outperforms the other baseline models in terms of generalization ability to larger systems and robustness to significant levels of noise.

The proposed methodology can generalize well to larger particle systems. However, we have to point out that the trained model cannot extrapolate the data arbitrarily far from the training distribution. In our experiments, we found that the edge neural network converges to linear functions outside the training input space. This observation matches the discussion in [37], which is an inherent limitation of MLPs.

The developed methodology will help to make a step forward in developing a flexible and robust tool for the discovery of physical laws in material mechanics. Such tools will be able to support, for example, additive manufacturing with heterogeneous materials that are particularly subject to highly varying material properties, *e.g.*, sustainable or recycled materials [38].

5 Methods

5.1 Notations and formal task description

We use a fully-connected directed graph G=(V,E) to represent the interacting particle system, where nodes $V=\{v_1,v_2,\ldots,v_{|V|}\}$ correspond to the particles and the directed edges $E=\{e_{ij}:v_i,v_j\in V,i\neq j\}$ correspond to particle interactions. Under this notation, v_i refers to the i-th particle, and e_{ij} is the directed edge from v_j to v_i . We use $\{\eta_i^t\}_{i,t}$ to denote the observation of particle states at different time steps, where η_i^t is a vector describing the state of particle v_i at time t. We note that $\eta_i^t\in\mathbb{R}^{2d+2}$ (d is the space dimension) includes position $r_i^t\in\mathbb{R}^d$, velocity $\dot{r}_i^t\in\mathbb{R}^d$, electric charge $q_i\in\mathbb{R}$ and mass $m_i\in\mathbb{R}$. The velocity \dot{r}_i^t and acceleration \ddot{r}_i^t at time t are computed from the position series of particle v_i . We use \mathcal{M}_{ij} to denote the message from v_j to v_i learnt by the neural network $\hat{G}_E(\cdot;\theta_E)$ with parameters θ_E . Our goal is to infer the pairwise force F_{ij}^t and the potential energy P_{ij}^t on every edge e_{ij} at each time t given the observation of particle trajectories.

5.2 PIG'N'PI details

PIG'N'PI contains an edge part to learn the pairwise interaction and a node part to aggregate the interactions to derive node accelerations (see Fig. 1). In the edge part, we use MLPs as universal approximators [39, 40] to learn the pairwise force or pairwise potential energy. We denote this edge neural network as $\hat{G}_E(\cdot;\theta_E)$. $\hat{G}_E(\cdot;\theta_E)$ takes the vectors η_i and η_j of two nodes as input. The output \mathcal{M}_{ij} of $\hat{G}_E(\cdot;\theta_E)$ is the inferred pairwise force \hat{F}_{ij} or potential energy \hat{P}_{ij} on edge e_{ij} , depending on the operator in the node part. We design the physics operator $G_N(\cdot)$ to aggregate the edge messages in the node part and derive the acceleration \hat{r}_i^t for every particle v_i at time t. We optimize parameters θ_E by minimizing the mean absolute error between the predicted acceleration and the true acceleration. The objective function is given by:

$$\arg\min_{\theta_E} \mathcal{L} = \frac{1}{|\mathcal{T}_{\text{train}}|} \frac{1}{|V|} \sum_{t \in \mathcal{T}_{\text{train}}} \sum_{i=1}^{|V|} l_1(\hat{\vec{r}}_i^t, \vec{r}_i^t)$$
(3)

In the following, we explain the design of the edge neural network $\hat{G}_E(\cdot; \theta_E)$ and the node part operator $G_N(\cdot)$ in two cases: inferring the pairwise force and inferring the pairwise potential energy.

Learning pairwise force

We use an MLP as the edge neural network $\hat{G}_E(\cdot;\theta_E)$ to learn the pairwise force from v_j to v_i on each edge e_{ij} . The output dimension of $\hat{G}_E(\cdot;\theta_E)$ is the same as the spatial dimension d. We first concatenate η_i^t and η_j^t which is the input of $\hat{G}_E(\cdot;\theta_E)$. We denote the corresponding output as $\mathcal{M}_{ij}^t \in \mathbb{R}^d$, e.g.,

$$\mathcal{M}_{ij}^{t} \triangleq \hat{G}_{E}(\operatorname{concat}(\boldsymbol{\eta}_{i}^{t}, \boldsymbol{\eta}_{j}^{t}); \theta_{E}) \tag{4}$$

According to Newton's Second law, the net acceleration of every particle is equal to the net force divided by its mass. Hence, in the node part of PIG'N'PI, we first sum up all incoming messages $\mathcal{M}_i = \sum_j^{j \neq i} \mathcal{M}_{ij}$ of every particle v_i , and then divide it by the mass of the particle m_i . The output of $G_N(\cdot)$ is the predicted acceleration \hat{r}_i on particle v_i :

$$\hat{\boldsymbol{r}}_{i}^{t} = G_{N}(\boldsymbol{\eta}_{i}^{t}, \mathcal{M}_{i}^{t})
= G_{N}(\boldsymbol{\eta}_{i}^{t}, \sum_{j}^{j \neq i} \mathcal{M}_{ij}^{t})
= \frac{\sum_{j}^{j \neq i} \mathcal{M}_{ij}^{t}}{m_{i}}$$
(5)

We optimize the parameters θ_E in $\hat{G}_E(\cdot;\theta_E)$ by minimizing the objective function Eq. (3). Through this process, the node part operator $G_N(\cdot)$ guides the edge neural network $\hat{G}_E(\cdot;\theta_E)$ to predict the pairwise force exactly, e.g.,

$$\hat{F}_{ij}^t = \mathcal{M}_{ij}^t \tag{6}$$

This is illustrated in Block (B) of Fig. 2.

Learning pairwise potential energy

For the pairwise potential energy case, the edge neural network $\hat{G}_E(\cdot;\theta_E)$ is designed to output the pairwise potential energy. Here, the output dimension of $\hat{G}_E(\cdot;\theta_E)$ is one because the potential energy is a scalar. We still first concatenate η_i^t and η_j^t as the input of $\hat{G}_E(\cdot;\theta_E)$ and use MLPs as $\hat{G}_E(\cdot;\theta_E)$. The corresponding output $\mathcal{M}_{ij}^t \in \mathbb{R}$ is denoted as:

$$\mathcal{M}_{ij}^{t} \triangleq \hat{G}_{E}(\operatorname{concat}(\boldsymbol{\eta}_{i}^{t}, \boldsymbol{\eta}_{i}^{t}); \theta_{E}) \tag{7}$$

We know that the net force of every particle equals to the negative partial derivative of the potential energy with respect to its position. Hence, in the node part, we first sum up all incoming messages $\mathcal{M}_i = \sum_j^{j \neq i} \mathcal{M}_{ij}$ for every particle i, then compute the negative derivative with respect to the input position and finally divide it by the mass. The final output corresponds then to the predicted acceleration. The node part operator $G_N(\cdot)$ for the potential energy case is given by:

$$\hat{\boldsymbol{r}}_{i}^{t} = G_{N}(\boldsymbol{\eta}_{i}^{t}, \mathcal{M}_{i}^{t})
= G_{N}(\boldsymbol{\eta}_{i}^{t}, \sum_{j}^{j \neq i} \mathcal{M}_{ij}^{t})
= -\frac{\partial (\sum_{j}^{j \neq i} \mathcal{M}_{ij}^{t})/\partial \boldsymbol{r}_{i}^{t}}{m_{i}}$$
(8)

Analogously to the force-based case, we optimize for the parameters θ_E in $\hat{G}_E(\cdot;\theta_E)$ by minimizing the acceleration loss (Eq. (3)). The node part operator $G_N(\cdot)$ here guides the edge neural network $\hat{G}_E(\cdot;\theta_E)$ to learn the pairwise potential energy exactly. The learnt message on each edge corresponds to the predicted pairwise potential energy, and the negative partial derivative is the predicted pairwise force, e.g.,

$$\hat{P}_{ij} = \mathcal{M}_{ij}$$

$$\hat{\mathbf{F}}_{ij} = -\partial \hat{P}_{ij}/\partial \mathbf{r}_i = -\partial \mathcal{M}_{ij}/\partial \mathbf{r}_i$$
(9)

This is illustrated in Block (C) of Fig. 2.

We note that the commonly used ReLU activation function is not suitable as activation function in $\hat{G}_E(\cdot;\theta_E)$ for learning the potential energy. The reason is that we compute the partial derivative of $\mathcal{M}_{ij} = \hat{G}_E(\operatorname{concat}(\eta_i,\eta_j);\theta_E)$ to derive the predicted accelerations for every particle. The derivative should be continuous and even smooth considering physical forces. However, ReLU approximates the underlying function by piece-wise linear hyper-planes with sharp boundaries. The first-order derivative is, thus, piece-wise constant that does not change with input [23]. Details on selecting the activation function in $\hat{G}_E(\cdot;\theta_E)$ are explained in Sec. 5.5.

5.3 Details on imposing a symmetry regularization on the baseline model

As mentioned in Sec. 3.5, to ensure that the model satisfies the action-reaction physical consistency requirement, we also test an extension of the baseline model by imposing a symmetry regularization on the corresponding pairwise messages in the baseline model. This can be considered as an alternative way of imposing physical consistency. In detail, let \mathcal{M}_{ij} be the message from v_j to v_i which is the output of the edge neural network of the baseline model. In our experimental setup, the message \mathcal{M}_{ij} corresponds to the force from v_j to v_i . We impose the symmetry regularization by adding a regularization term on the learnt messages in the objective function (Eq. (3)). This results in the following objective function:

$$\arg\min_{\theta_{E}} \mathcal{L} = \frac{1}{|\mathcal{T}_{\text{train}}|} \sum_{t \in \mathcal{T}_{\text{train}}} \left(\underbrace{\frac{1}{|V|} \sum_{i=1}^{|V|} |\hat{\vec{r}}_{i}^{t} - \ddot{\vec{r}}_{i}^{t}|}_{\text{Acceleration loss on nodes}} + \underbrace{\alpha \frac{1}{|E|} \sum_{i,j}^{i \neq j} |\mathcal{M}_{ij}^{t} + \mathcal{M}_{ji}^{t}|}_{\text{Symmetry regularization loss on edges}} \right)$$
(10)

where α is a weight parameter. The original baseline model can be considered as the special case with $\alpha = 0$ in Eq. (10). In our experiments, we evaluate the impact of the regularization term with different weights ($\alpha = 0.1, 1.0, 10, 100$). The results are reported in SI Table 11.

5.4 Details of the method to learn pairwise force introduced by [33]

Lemos et al. [33] proposed a method that has a similar goal to the proposed PIG'N'PI applied to pairwise force prediction. The authors also impose Newton's second law in the standard GN block by dividing the aggregated messages by the node property. We denote this method as GN+. The main difference between GN+ and PIG'N'PI is that GN+ treats the node property as a learnable parameter. It assigns an individual learnable scalar w_i for each particle v_i and predicts the acceleration of v_i by dividing the aggregated incoming messages by 10^{w_i} . The learnable scalars on all nodes representing the pairwise force are learnt together with all other parameters. It is important to point out that GN+ was designed solely for learning the pairwise force while PIG'N'PI can be applied both: to infer the pairwise forces and also the pairwise potential energy. The detailed results of GN+ are reported in Table 3, Table 5, Table 7, Fig. 3D, Fig. 4 and Fig. 8.

5.5 Details about simulation and experiments

Here, we summarize the different force functions used in our simulation. Please note that in this work, we used the same case studies as in previous work [24]. However, we adapted the parameters of the particle systems slightly to make the learning more challenging.

- Spring force We denote the spring constant as k and balance length as L. The pairwise force from v_i to v_j is $k(r_{ij}-L)\boldsymbol{n}_{ij}$ and its potential energy is $0.5k(r_{ij}-L)^2$, where $r_{ij}=\|\boldsymbol{r}_j-\boldsymbol{r}_i\|$ is the Euclidean distance and $\boldsymbol{n}_{ij}=\frac{\boldsymbol{r}_j-\boldsymbol{r}_i}{\|\boldsymbol{r}_j-\boldsymbol{r}_i\|}$ is the unit vector pointing from v_i to v_j . We set k=2.0 and L=1.0 in our simulations.
- Charge force The electric charge force from v_i to v_j is $-cq_iq_jn_{ij}/r_{ij}^2$ and the potential energy is cq_iq_j/r_{ij} , where c is the charge constant, and q_i,q_j are the electric charges. We set c=1.0 in the simulation. Furthermore, to prevent any zeros in the denominator, we add a small number δ ($\delta=0.01$) when computing distances.

- Orbital force The orbital force from v_i to v_j equals to $m_i m_j n_{ij}/r_{ij}$ and the potential energy is $m_i m_j \ln(r_{ij})$, where m_i, m_j are the masses of v_i and v_j . We again add a small number δ ($\delta = 0.01$) when computing distances to prevent zeros in the denominator and logarithm.
- **Discontinuous force** We set threshold constant $\Theta = 2.0$ such that the pairwise force is $\mathbf{0}$ if the Euclidean distance r_{ij} is strictly smaller than this threshold and $(r_{ij} 1)\mathbf{n}_{ij}$ otherwise. The corresponding potential is 0 if r_{ij} is strictly smaller than this threshold and $0.5(r_{ij} 1)^2$ otherwise.

We intentionally omit units for variables because the simulation data can be at arbitrary scale. Moreover, the presented cases serve as proof of concept to learn the input–output relation. Further, we note that m_i is sampled from the log-uniform distribution within the range [-1] ($\ln(m_i) \sim \mathcal{U}(-1,1)$). q_i is uniformly sampled from the range [-1,1]. Initial location and velocity of particles are both sampled from the normal Gaussian distribution $\mathcal{N}(0,1)$. Each simulation contains eight particles. Each particle is associated with the corresponding features including position, velocity, mass and charge. The target for prediction is node accelerations. Every simulation contains 10,000 time steps with step size 0.01. We randomly split the simulation steps into training dataset, validation dataset and testing dataset with the ratio 7:1.5:1.5. We use $\mathcal{T}_{\text{train}}$, $\mathcal{T}_{\text{valid}}$ and $\mathcal{T}_{\text{test}}$ to indicate the simulation time steps corresponding to training split, validation split and testing split. We train the model on the training dataset (optimizing the parameters θ_E in $\hat{G}_E(\cdot;\theta_E)$) by optimizing Eq. (3), fine-tune hyperparameters and select the best trained model on the validation dataset and report the performance of the selected trained model on the testing dataset. For generalization tests, we re-run each simulation on 12 particles with 1500 time steps (same size as original testing dataset). The previously selected trained model with eight particles is tested on the new testing dataset.

We only fine-tune hyperparameters on the spring validation dataset and use the same hyperparameters in all experiments. We set the learning rate to 0.001, the number of hidden layers in the edge neural network to four, the units of hidden layers to 300, max training epochs to 200. The dimension of the output layer in the edge neural network is d to learn the force or one to learn the potential energy. We use the Adam optimizer with the mini-batch size of 32 for the force case study and eight for the potential case study to train the model. The SiLU activation function is used in all PIG'N'PI evaluations.

6 Data availability

The data used in the experiments are generated by the numerical simulator. All data used for the experiments are included in the associated Gitlab repository: https://gitlab.ethz.ch/cmbm-public/pignpi/-/tree/main/simulation.

7 Code availability

The implementation of PIG'N'PI is based on PyTorch [41] and pytorch-geometric [42] libraries. The source code is available on Gitlab: https://gitlab.ethz.ch/cmbm-public/pignpi.

8 Acknowledgements

This project has been funded by the ETH Grant office. The contribution of Olga Fink to this project was funded by the Swiss National Science Foundation (SNSF) Grant no. PP00P2_176878.

9 Author contributions

DK and OF conceptualized the idea, ZH developed the methodology, ZH, DK and OF conceived the experiments, ZH conducted the experiments, ZH, DK and OF analysed the results, and all authors wrote the manuscript.

10 Competing interests.

The authors declare no competing interest.

References

- [1] Carl D Murray and Stanley F Dermott. *Solar system dynamics*. Cambridge university press, 1999.
- [2] Francesco Dramis. Mass movement processes and landforms. *International Encyclopedia of Geography: People, the Earth, Environment and Technology: People, the Earth, Environment and Technology*, pages 1–9, 2016.
- [3] W Gregory Sawyer, Nicolas Argibay, David L Burris, and Brandon A Krick. Mechanistic studies in friction and wear of bulk materials. *Annual Review of Materials Research*, 44:395–427, 2014.
- [4] Edward P Furlani. Magnetic biotransport: analysis and applications. *Materials*, 3(4):2412–2446, 2010.
- [5] Wujie Wang and Rafael Gómez-Bombarelli. Coarse-graining auto-encoders for molecular dynamics. *npj Computational Materials*, 5(1):1–9, 2019.
- [6] Stefano Angioletti-Uberti. Theory, simulations and the design of functionalized nanoparticles for biomedical applications: a soft matter perspective. *npj Computational Materials*, 3(1):1–15, 2017.
- [7] Alexander Radovic, Mike Williams, David Rousseau, Michael Kagan, Daniele Bonacorsi, Alexander Himmel, Adam Aurisano, Kazuhiro Terao, and Taritree Wongjirad. Machine learning at the energy and intensity frontiers of particle physics. *Nature*, 560(7716):41–48, 2018.
- [8] Giuseppe Carleo, Ignacio Cirac, Kyle Cranmer, Laurent Daudet, Maria Schuld, Naftali Tishby, Leslie Vogt-Maranto, and Lenka Zdeborová. Machine learning and the physical sciences. *Reviews of Modern Physics*, 91(4):045002, 2019.
- [9] Jie Zhou, Ganqu Cui, Shengding Hu, Zhengyan Zhang, Cheng Yang, Zhiyuan Liu, Lifeng Wang, Changcheng Li, and Maosong Sun. Graph neural networks: A review of methods and applications. *AI Open*, 1:57–81, 2020.
- [10] Jonathan Shlomi, Peter Battaglia, and Jean-Roch Vlimant. Graph neural networks in particle physics. *Machine Learning: Science and Technology*, 2(2):021001, 2020.
- [11] Kenneth Atz, Francesca Grisoni, and Gisbert Schneider. Geometric deep learning on molecular representations. *Nature Machine Intelligence*, 3(12):1023–1032, 2021.
- [12] Oscar Méndez-Lucio, Mazen Ahmad, Ehecatl Antonio del Rio-Chanona, and Jörg Kurt Wegner. A geometric deep learning approach to predict binding conformations of bioactive molecules. *Nature Machine Intelligence*, 3(12):1033–1039, 2021.
- [13] Cheol Woo Park, Mordechai Kornbluth, Jonathan Vandermause, Chris Wolverton, Boris Kozinsky, and Jonathan P. Mailoa. Accurate and scalable graph neural network force field and molecular dynamics with direct force architecture. *npj Computational Materials*, 7(1):73, 2021.
- [14] Alvaro Sanchez-Gonzalez, Jonathan Godwin, Tobias Pfaff, Rex Ying, Jure Leskovec, and Peter Battaglia. Learning to simulate complex physics with graph networks. In *International Conference on Machine Learning (ICML)*, pages 8459–8468. PMLR, 2020.
- [15] Shigeyuki Matsumoto, Shoichi Ishida, Mitsugu Araki, Takayuki Kato, Kei Terayama, and Yasushi Okuno. Extraction of protein dynamics information from cryo-em maps using deep learning. *Nature Machine Intelligence*, 3(2):153–160, 2021.
- [16] Kristof T Schütt, Pieter-Jan Kindermans, Huziel E Sauceda, Stefan Chmiela, Alexandre Tkatchenko, and Klaus-Robert Müller. Schnet: A continuous-filter convolutional neural network for modeling quantum interactions. In *Proceedings of the 31st International Conference on Neural Information Processing Systems (NeurIPS)*, page 992–1002, 2017.

- [17] Kristof T Schütt, Huziel E Sauceda, P-J Kindermans, Alexandre Tkatchenko, and K-R Müller. Schnet–a deep learning architecture for molecules and materials. *The Journal of Chemical Physics*, 148(24):241722, 2018.
- [18] Thomas Kipf, Ethan Fetaya, Kuan-Chieh Wang, Max Welling, and Richard Zemel. Neural relational inference for interacting systems. In *International Conference on Machine Learning (ICML)*, pages 2688–2697. PMLR, 2018.
- [19] Oliver T Unke and Markus Meuwly. Physnet: A neural network for predicting energies, forces, dipole moments, and partial charges. *Journal of chemical theory and computation*, 15(6): 3678–3693, 2019.
- [20] Johannes Klicpera, Janek Groß, and Stephan Günnemann. Directional message passing for molecular graphs. In *International Conference on Learning Representations (ICLR)*, 2020.
- [21] Johannes Klicpera, Shankari Giri, Johannes T Margraf, and Stephan Günnemann. Fast and uncertainty-aware directional message passing for non-equilibrium molecules. In *Machine Learning for Molecules Workshop* @ *NeurIPS*, 2020.
- [22] Victor Bapst, Thomas Keck, A Grabska-Barwińska, Craig Donner, Ekin Dogus Cubuk, Samuel S Schoenholz, Annette Obika, Alexander WR Nelson, Trevor Back, Demis Hassabis, et al. Unveiling the predictive power of static structure in glassy systems. *Nature Physics*, 16(4): 448–454, 2020.
- [23] Weihua Hu, Muhammed Shuaibi, Abhishek Das, Siddharth Goyal, Anuroop Sriram, Jure Leskovec, Devi Parikh, and C Lawrence Zitnick. Forcenet: A graph neural network for large-scale quantum calculations. arXiv preprint arXiv:2103.01436, 2021.
- [24] Miles Cranmer, Alvaro Sanchez Gonzalez, Peter Battaglia, Rui Xu, Kyle Cranmer, David Spergel, and Shirley Ho. Discovering symbolic models from deep learning with inductive biases. In *Advances in Neural Information Processing Systems (NeurIPS)*, volume 33, pages 17429–17442, 2020.
- [25] Peter W Battaglia, Jessica B Hamrick, Victor Bapst, Alvaro Sanchez-Gonzalez, Vinicius Zambaldi, Mateusz Malinowski, Andrea Tacchetti, David Raposo, Adam Santoro, Ryan Faulkner, et al. Relational inductive biases, deep learning, and graph networks. *arXiv preprint arXiv:1806.01261*, 2018.
- [26] Samuel Greydanus, Misko Dzamba, and Jason Yosinski. Hamiltonian neural networks. In *Advances in Neural Information Processing Systems (NeurIPS)*, volume 32, 2019.
- [27] Alvaro Sanchez-Gonzalez, Victor Bapst, Kyle Cranmer, and Peter Battaglia. Hamiltonian graph networks with ode integrators. In *Machine Learning and the Physical Sciences Workshop* @ *NeurIPS*, 2019.
- [28] Michael Lutter, Christian Ritter, and Jan Peters. Deep lagrangian networks: Using physics as model prior for deep learning. In *International Conference on Learning Representations* (*ICLR*), 2019.
- [29] Jiang Wang, Simon Olsson, Christoph Wehmeyer, Adrià Pérez, Nicholas E Charron, Gianni De Fabritiis, Frank Noé, and Cecilia Clementi. Machine learning of coarse-grained molecular dynamics force fields. ACS central science, 5(5):755–767, 2019.
- [30] Marc Finzi, Ke Alexander Wang, and Andrew G Wilson. Simplifying hamiltonian and lagrangian neural networks via explicit constraints. In *Advances in neural information processing systems* (*NeurIPS*), volume 33, pages 13880–13889, 2020.
- [31] George Em Karniadakis, Ioannis G Kevrekidis, Lu Lu, Paris Perdikaris, Sifan Wang, and Liu Yang. Physics-informed machine learning. *Nature Reviews Physics*, 3(6):422–440, 2021.
- [32] Ian Goodfellow, Yoshua Bengio, and Aaron Courville. Deep learning. MIT press, 2016.
- [33] Pablo Lemos, Niall Jeffrey, Miles Cranmer, Peter Battaglia, and Shirley Ho. Rediscovering newton's gravity and solar system properties using deep learning and inductive biases. In *SimDL Workshop @ ICLR*, 2021.

- [34] Zijie Li, Kazem Meidani, Prakarsh Yadav, and Amir Barati Farimani. Graph neural networks accelerated molecular dynamics. *The Journal of Chemical Physics*, 156(14):144103, 2022.
- [35] Dennis C Rapaport and Dennis C Rapaport Rapaport. *The art of molecular dynamics simulation*. Cambridge university press, 2004.
- [36] Sina Amini Niaki, Ehsan Haghighat, Trevor Campbell, Anoush Poursartip, and Reza Vaziri. Physics-informed neural network for modelling the thermochemical curing process of composite-tool systems during manufacture. *Computer Methods in Applied Mechanics and Engineering*, 384:113959, 2021.
- [37] Keyulu Xu, Mozhi Zhang, Jingling Li, Simon Shaolei Du, Ken-Ichi Kawarabayashi, and Stefanie Jegelka. How neural networks extrapolate: From feedforward to graph neural networks. In *International Conference on Learning Representations (ICLR)*, 2021.
- [38] Qi Wang and Longfei Zhang. Inverse design of glass structure with deep graph neural networks. *Nature Communications*, 12(1):5359, 2021.
- [39] Kurt Hornik, Maxwell Stinchcombe, and Halbert White. Multilayer feedforward networks are universal approximators. *Neural networks*, 2(5):359–366, 1989.
- [40] Kurt Hornik. Approximation capabilities of multilayer feedforward networks. *Neural networks*, 4(2):251–257, 1991.
- [41] Adam Paszke, Sam Gross, Soumith Chintala, Gregory Chanan, Edward Yang, Zachary DeVito, Zeming Lin, Alban Desmaison, Luca Antiga, and Adam Lerer. Automatic differentiation in pytorch. In *Workshop on Autodiff @ NeurIPS*, 2017.
- [42] Matthias Fey and Jan E. Lenssen. Fast graph representation learning with PyTorch Geometric. In *Representation Learning on Graphs and Manifolds Workshop* @ *ICLR*, 2019.

A Supplementary information

A.1 Symbol table

The variable notations used in the paper are summarized in Table 2.

Table 2: Symbol notations and their meanings

notation	meaning
G = (V, E)	graph representation of the interacting particle system
$V = \{v_1, v_2, \dots, v_{ V }\}$	set of nodes corresponding to particles
$E = \{e_{ij} : v_i, v_j \in V, i \neq j\}$	set of edges corresponding to interactions between particles
$v_i \in V$	i-th particle
$e_{ij} \in E$	directed edge from particle v_j to particle v_i
d	spatial dimension (2 or 3)
$oldsymbol{r}_i^t \in \mathbb{R}^d$	position of v_i at time t
$oldsymbol{n}_{ij} \in \mathbb{R}^d$	unit vector pointing from v_i to v_j , $m{n}_{ij} = \frac{m{r}_j - m{r}_i}{\left\ m{r}_j - m{r}_i \right\ }$
$oldsymbol{\dot{r}}_i^t \in \mathbb{R}^d$	velocity of v_i at time t
$q_i \in \mathbb{R}$	electric charge of particle v_i , it is a constant
$m_i \in \mathbb{R}$	mass of particle v_i , it is a constant
$oldsymbol{\eta}_i^t \in \mathbb{R}^{2d+2}$	feature vector of particle v_i at time t , $\boldsymbol{\eta}_i^t = [\boldsymbol{r}_i^t, \dot{\boldsymbol{r}}_i^t, q_i, m_i]$
$m{\ddot{r}}_i^t \in \mathbb{R}^d$	true acceleration of particle v_i at time t
$\boldsymbol{\hat{\ddot{r}}}_i^t \in \mathbb{R}^d$	predicted acceleration of particle v_i at time t
$oldsymbol{F}_{ij}^t \in \mathbb{R}^d$	true force from v_j to v_i at time t
$\hat{m{F}}_{ij}^t \in \mathbb{R}^d$	predicted force from v_j to v_i at time t
$P_{ij}^t \in \mathbb{R}$	true potential energy incurred by v_j on v_i at time t
$\hat{P}_{ij}^t \in \mathbb{R}$	predicted potential energy incurred by v_j on v_i at time t
$\hat{G}_E(\cdot; heta_E)$	edge part neural network of PIG'N'PI with learnable parameters θ_E
$G_N(\cdot)$	proposed deterministic node part operator of PIG'N'PI
$ heta_E$	learnable parameters in the edge neural network $\hat{G}_E(\cdot; heta_E)$
\mathcal{M}_{ij}	learnt message from v_j to v_i output by edge neural network $\hat{G}_E(\cdot; \theta_E)$,
	$\mathcal{M}_{ij} \in \mathbb{R}^d$ in learning force and $\mathcal{M}_{ij} \in \mathbb{R}$ in learning potential
\mathcal{M}_i	sum of all incoming message on particle v_i , $\mathcal{M}_i = \sum_i^{j \neq i} \mathcal{M}_{ij}$
$\mathcal{T}_{ ext{train}}$	set of time steps corresponding to the training split of simulation data
T _{valid}	set of time steps corresponding to the validation split of simulation data
$\mathcal{T}_{ ext{test}}$	set of time steps corresponding to the testing split of simulation data
$l_1(x,y)$	sum of absolute differences between each element in x and y , $l_1(x, y) = \sum_i x_i - y_i $, if x and y are vectors; or the absolute difference, $l_1(x, y) = \sum_i x_i - y_i $
$\iota_1(x,y)$	x-y , if if x and y are scalars
k	stiffness constant in spring simulation, we set $k=2$
L	balance length constant in spring simulation, we set $L=1$
c	constant in charge simulation, we set $c=1$
Θ	threshold constant in discontinuous dataset simulation, we set $\Theta = 2$
_	The second of th

A.2 Performance evaluation of learning physics-consistent particle interactions (force and potential energy)

Two different performance characteristics are evaluated. First, the learning performance is evaluated and, second, the ability of the algorithms to learn the particle interactions that are consistent with the underlying physical laws.

We compute the following metrics for evaluating the performance of PIG'N'PI and the baseline model to learn the pairwise force:

$$\mathsf{MAE}_{\mathsf{acc}} = \mathsf{MAE}^{\mathsf{part}}(\hat{\boldsymbol{r}}, \boldsymbol{r}) = \frac{1}{|\mathcal{T}_{\mathsf{test}}|} \frac{1}{|V|} \sum_{t \in \mathcal{T}_{\mathsf{test}}} \sum_{i \in V} l_1(\hat{\boldsymbol{r}}_i^t, \boldsymbol{r}_i^t)$$
(11)

$$\mathsf{MAE}_{\mathsf{ef}} = \mathsf{MAE}^{\mathrm{inter}}(\hat{\boldsymbol{F}}, \boldsymbol{F}) = \frac{1}{|\mathcal{T}_{\mathsf{test}}|} \frac{1}{|E|} \sum_{t \in \mathcal{T}_{\mathsf{test}}} \sum_{i,j \in V}^{i \neq j} l_1(\hat{\boldsymbol{F}}_{ij}^t, \boldsymbol{F}_{ij}^t)$$
(12)

$$\mathsf{MAE}_{\mathsf{nf}} = \mathsf{MAE}^{\mathsf{part}}(\hat{\boldsymbol{F}}, \boldsymbol{F}) = \frac{1}{|\mathcal{T}_{\mathsf{test}}|} \frac{1}{|V|} \sum_{t \in \mathcal{T}_{\mathsf{test}}} \sum_{i \in V} l_1(\hat{\boldsymbol{F}}_i^t, \boldsymbol{F}_i^t), \text{ where } \hat{\boldsymbol{F}}_i^t = \sum_{j}^{j \neq i} \hat{\boldsymbol{F}}_{ij}^t$$
(13)

$$\mathsf{MAE}_{\mathsf{symm}}^{F} = \frac{1}{|\mathcal{T}_{\mathsf{test}}|} \frac{1}{|E|} \sum_{t \in \mathcal{T}_{\mathsf{test}}} \sum_{i,j \in V}^{i \neq j} l_1(\hat{F}_{ij}^t, -\hat{F}_{ji}^t) \tag{14}$$

where \ddot{r} and F are the ground-truth acceleration and force, and \hat{r} and \hat{F} are the predicted acceleration and force. Table 3 reports the performance of the baseline model and PIG'N'PI to the learn pairwise force in terms of metrics listed above (learning performance and the ability of the algorithms to learn physics-consistent particle interactions).

We use the following metrics for evaluating the performance to learn pairwise potential energy:

$$\mathsf{MAE}_{\mathsf{acc}} = \mathsf{MAE}^{\mathsf{part}}(\hat{\boldsymbol{r}}, \boldsymbol{\dot{r}}) = \frac{1}{|\mathcal{T}_{\mathsf{test}}|} \frac{1}{|V|} \sum_{t \in \mathcal{T}_{\mathsf{test}}} \sum_{i \in V} l_1(\hat{\boldsymbol{r}}_i^t, \boldsymbol{\ddot{r}}_i^t)$$
(15)

$$\mathsf{MAE}_{\Delta \mathsf{ep}} = \mathsf{MAE}^{\mathrm{inter}}(\hat{P} - \hat{P}^{0}, P - P^{0}) = \frac{1}{|\mathcal{T}_{\mathsf{test}}|} \frac{1}{|E|} \sum_{t \in \mathcal{T}_{\mathsf{est}}} \sum_{i,j \in V}^{i \neq j} l_{1}(\hat{P}_{ij}^{t} - \hat{P}_{ij}^{0}, P_{ij}^{t} - P_{ij}^{0}) \quad (16)$$

$$\mathsf{MAE}_{\Delta\mathsf{np}} = \mathsf{MAE}^{\mathsf{part}}(\hat{P} - \hat{P}^{0}, P - P^{0}) = \frac{1}{|\mathcal{T}_{\mathsf{test}}|} \frac{1}{|V|} \sum_{t \in \mathcal{T}_{\mathsf{test}}} \sum_{i \in |V|} l_{1} (\sum_{j}^{j \neq i} \hat{P}_{ij}^{t} - \sum_{j}^{j \neq i} \hat{P}_{ij}^{0}, P_{i}^{t} - P_{i}^{0})$$
(17)

$$\mathsf{MAE}_{\mathsf{ef}} = \mathsf{MAE}^{\mathrm{inter}}(\hat{\boldsymbol{F}}, \boldsymbol{F}) = \frac{1}{|\mathcal{T}_{\mathsf{test}}|} \frac{1}{|E|} \sum_{t \in \mathcal{T}_{\mathsf{ert}}} \sum_{i,j \in V}^{i \neq j} l_1(\hat{\boldsymbol{F}}_{ij}^t, \boldsymbol{F}_{ij}^t), \text{ where } \hat{\boldsymbol{F}}_{ij}^t = -\frac{\partial \hat{P}_{ij}^t}{\partial \boldsymbol{r}_i^t}$$
(18)

$$\mathsf{MAE}_{\mathsf{nf}} = \mathsf{MAE}^{\mathsf{part}}(\hat{\boldsymbol{F}}, \boldsymbol{F}) = \frac{1}{|\mathcal{T}_{\mathsf{test}}|} \frac{1}{|V|} \sum_{t \in \mathcal{T}_{\mathsf{ord}}} \sum_{i \in V} l_1(\hat{\boldsymbol{F}}_i^t, \boldsymbol{F}_i^t), \text{ where } \hat{\boldsymbol{F}}_i^t = -\frac{\partial \sum_{j}^{j \neq i} \hat{P}_{ij}^t}{\partial \boldsymbol{r}_i^t}$$
(19)

$$\mathsf{MAE}_{\mathsf{symm}}^{P} = \frac{1}{|\mathcal{T}_{\mathsf{test}}|} \frac{1}{|E|} \sum_{t \in \mathcal{T}_{\mathsf{test}}} \sum_{i,j \in V}^{i \neq j} l_1(\hat{P}_{ij}^t, \hat{P}_{ji}^t) \tag{20}$$

where \ddot{r} , F and P are the ground-truth accelerations, forces and potentials, \hat{r} , \hat{F} and \hat{P} are the predictions computed from Eq. (8)-(9). Table 4 reports the performance of baseline model and PIG'N'PI to learn pairwise potential energy.

Table 3: Performance of PIG'N'PI and the baseline model on pairwise force prediction. Baseline_{SiLU} denotes the baseline with the SiLU activation function. GN+ is the method to learn pairwise force introduced by [33]. Results averaged across five experiments.

		Spring dim=2	Spring dim=3	Charge dim=2	Charge dim=3	Orbital dim=2	Orbital dim=3	Discnt dim=2	Discnt dim=3
	Baseline	$0.0565 \\ \pm 0.0023$	$0.1076 \\ \pm 0.0012$	$0.2521 \\ \pm 0.0173$	$0.3824 \\ \pm 0.0559$	$0.0437 \\ \pm 0.0026$	$0.0439 \\ \pm 0.0014$	$0.0592 \\ \pm 0.0015$	$\begin{array}{c} 0.1171 \\ \pm 0.0010 \end{array}$
MAE _{acc}	Baseline _{SiLU}	$\begin{array}{c} 0.0258 \\ \scriptstyle{\pm 0.0011} \end{array}$	$\begin{array}{c} 0.0476 \\ \pm 0.0025 \end{array}$	$\begin{array}{c} 1.0326 \\ \pm 1.3788 \end{array}$	$\begin{array}{c} 0.2092 \\ \pm 0.0060 \end{array}$	$\begin{array}{c} 0.0187 \\ \scriptstyle{\pm 0.0005} \end{array}$	$\begin{array}{c} 0.0196 \\ \pm 0.0002 \end{array}$	$0.0249 \atop \pm 0.0002$	$0.0508 \\ \pm 0.0010$
	GN+	$\begin{array}{c} 0.0246 \\ \scriptstyle{\pm 0.0047} \end{array}$	$\begin{array}{c} 0.0542 \\ \pm 0.0047 \end{array}$	$\begin{array}{c} 0.1216 \\ \scriptstyle{\pm 0.0099} \end{array}$	$\begin{array}{c} 0.1890 \\ \scriptstyle{\pm 0.0111} \end{array}$	$\begin{array}{c} 0.0255 \\ \scriptstyle{\pm 0.0023} \end{array}$	$\begin{array}{c} 0.0581 \\ \scriptstyle{\pm 0.0004} \end{array}$	$\begin{array}{c} 0.0667 \\ \scriptstyle{\pm 0.0174} \end{array}$	$\begin{array}{c} 0.2280 \\ \scriptstyle{\pm 0.0951} \end{array}$
	PIG'N'PI	0.0206 ±0.0009	$\begin{array}{c} \textbf{0.0278} \\ \pm \textbf{0.0021} \end{array}$	$\begin{array}{c} \textbf{0.0425} \\ \pm \textbf{0.0053} \end{array}$	$\begin{array}{c} \textbf{0.1191} \\ \pm \textbf{0.0027} \end{array}$	0.0202 ±0.0003	$\begin{array}{c} \textbf{0.0182} \\ \pm \textbf{0.0003} \end{array}$	$\begin{array}{c} \textbf{0.0227} \\ \pm \textbf{0.0019} \end{array}$	0.0399 ±0.0011
	Baseline	$\substack{2.3979 \\ \pm 0.2095}$	$\begin{array}{c} 3.8952 \\ \pm 0.7178 \end{array}$	$\begin{array}{c} 1.1832 \\ \pm 0.0955 \end{array}$	$\begin{array}{c} 0.6447 \\ \pm 0.1118 \end{array}$	$\begin{array}{c} 4.1010 \\ \pm 0.1467 \end{array}$	$\begin{array}{c} 3.5379 \\ \pm 0.7571 \end{array}$	$\begin{array}{c} 1.6536 \\ \pm 0.0640 \end{array}$	$^{2.5803}_{\pm 0.2886}$
MAE_{ef}	Baseline _{SiLU}	4.2027 ±1.1242	$\begin{array}{c} 5.5185 \\ \pm 1.1452 \end{array}$	$\begin{array}{c} 2.1581 \\ \scriptstyle{\pm 0.9572} \end{array}$	$\begin{array}{c} 1.3842 \\ \scriptstyle{\pm 0.1411} \end{array}$	$\begin{array}{c} 3.1097 \\ \scriptstyle{\pm 0.7148} \end{array}$	$\begin{array}{c} 1.9863 \\ \scriptstyle{\pm 0.1434} \end{array}$	$\begin{array}{c} 2.6576 \\ \scriptstyle{\pm 0.4146} \end{array}$	$\substack{4.4222 \\ \pm 0.6116}$
	GN+	$0.5724 \\ \pm 0.2321$	$0.3638 \\ \pm 0.3133$	$\begin{array}{c} 1.0248 \\ \scriptstyle{\pm 0.0182} \end{array}$	$\begin{array}{c} 0.3137 \\ \scriptstyle{\pm 0.0051} \end{array}$	$\begin{array}{c} 0.9372 \\ \scriptstyle{\pm 0.0294} \end{array}$	$\begin{array}{c} 0.6943 \\ \scriptstyle{\pm 0.0661} \end{array}$	$0.3714 \\ \scriptstyle{\pm 0.2711}$	$0.6974 \\ \pm 0.4143$
	PIG'N'PI	$\begin{array}{c} \textbf{0.0063} \\ \pm \textbf{0.0002} \end{array}$	$\begin{array}{c} \textbf{0.0101} \\ \pm \textbf{0.0007} \end{array}$	$\begin{array}{c} \textbf{0.0136} \\ \pm \textbf{0.0023} \end{array}$	$\begin{array}{c} \textbf{0.0363} \\ \pm \textbf{0.0015} \end{array}$	$\begin{array}{c} \textbf{0.0093} \\ \pm \textbf{0.0002} \end{array}$	$\begin{array}{c} \textbf{0.0095} \\ \pm \textbf{0.0001} \end{array}$	$\begin{array}{c} \textbf{0.0040} \\ \pm \textbf{0.0004} \end{array}$	$\begin{array}{c} \textbf{0.0079} \\ \pm 0.0002 \end{array}$
	Baseline	$^{11.652}_{\pm 0.9890}$	$\begin{array}{c} 20.967 \\ \pm 3.8552 \end{array}$	$\begin{array}{c} 6.8310 \\ \scriptstyle{\pm 0.5548} \end{array}$	$\begin{array}{c} 3.8038 \\ \pm 0.7523 \end{array}$	$18.194 \atop \pm 0.6884$	$16.677 \\ \pm 3.5212$	$10.786 \atop \pm 0.3764$	$15.651 \atop \pm 1.7983$
MAE_{nf}	Baseline _{SiLU}	20.685 ±5.0491	$\begin{array}{c} 29.824 \\ \pm 6.2007 \end{array}$	$\begin{array}{c} 12.480 \\ \scriptstyle{\pm 5.4145} \end{array}$	$\begin{array}{c} 8.7533 \\ \pm 0.9595 \end{array}$	$13.644 \\ \pm 3.1699$	$\begin{array}{c} 9.2546 \\ \pm 0.6675 \end{array}$	$\begin{array}{c} 17.430 \\ \scriptstyle{\pm 2.7127} \end{array}$	$\begin{array}{c} 27.149 \\ \pm 3.8191 \end{array}$
	GN+	2.7639 ±1.1198	$1.9370 \\ \scriptstyle{\pm 1.6941}$	$\begin{array}{c} 5.9332 \\ \pm 0.1038 \end{array}$	$^{1.6546}_{\pm 0.0299}$	3.9950 ±0.1166	$\begin{array}{c} 3.1841 \\ \pm 0.2858 \end{array}$	$\underset{\pm 1.8009}{2.4280}$	4.2270 ±2.6246
	PIG'N'PI	0.0219 ±0.0010	$\begin{array}{c} \textbf{0.0292} \\ \pm \textbf{0.0022} \end{array}$	$\begin{array}{c} \textbf{0.0488} \\ \pm \textbf{0.0059} \end{array}$	$\begin{array}{c} \textbf{0.1317} \\ \pm \textbf{0.0033} \end{array}$	0.0260 ±0.0005	$\begin{array}{c} \textbf{0.0233} \\ \pm \textbf{0.0004} \end{array}$	0.0239 ±0.0020	0.0419 ±0.0011
E	Baseline	1.1099 ± 0.0785	$1.7452 \atop \pm 0.0467$	$\begin{array}{c} 0.1248 \\ \pm 0.0137 \end{array}$	$0.6938 \\ \pm 0.2670$	$\substack{2.2074 \\ \pm 0.1852}$	$1.7684 \atop \pm 0.0941$	$0.9399 \\ \pm 0.0257$	$^{1.4118}_{\pm 0.0722}$
MAE^F_symm	Baseline _{SiLU}	2.1473 ±0.1366	3.1809 ±0.5156	2.1585 ±1.8080	$\substack{2.1378 \\ \pm 0.2803}$	0.8103 ±0.1062	$0.8877 \\ \pm 0.0584$	1.6121 ±0.2357	2.4231 ±0.3908
	GN+	0.0400 ±0.0437	0.0756 ±0.0284	0.1013 ±0.0082	0.0315 ±0.0033	1.0831 ±0.0733	0.8068 ±0.1251	0.0102 ±0.0041	0.0975 ±0.0927
	PIG'N'PI	0.0075 ±0.0003	0.0133 ±0.0008	0.0185 ±0.0036	0.0345 ±0.0017	0.0136 ±0.0004	0.0134 ±0.0004	0.0026 ±0.0004	0.0066 ±0.0001

Table 4: Performance evaluation of PIG'N'PI and the baseline model on the pairwise potential energy learning task. Baseline $_{SiLU}$ denotes the baseline model with SiLU activation function. We report the error of predicting the potential energy and its first-order derivative which corresponds to the inter-particle force. Results averaged across five experiments.

		Spring dim=2	Spring dim=3	Charge dim=2	Charge dim=3	Orbital dim=2	Orbital dim=3	Discnt dim=2	Discnt dim=3
MAE _{acc}	Baseline	$^{1.4841}_{\pm 0.0064}$	$\begin{array}{c} 1.9996 \\ \pm 0.0253 \end{array}$	$\begin{array}{c} 2.9127 \\ \pm 0.0844 \end{array}$	$\begin{array}{c} 0.5959 \\ \pm 0.0087 \end{array}$	$\substack{2.4585 \\ \pm 0.0399}$	$^{1.0113}_{\pm 0.0100}$	$\begin{array}{c} 0.4532 \\ \scriptstyle{\pm 0.0186} \end{array}$	$\begin{array}{c} 0.7222 \\ \scriptstyle{\pm 0.0168} \end{array}$
······-acc	Baseline _{SiLU}	$\begin{array}{c} 1.4094 \\ \pm 0.0842 \end{array}$	$\begin{array}{c} 1.8721 \\ \pm 0.0567 \end{array}$	$\begin{array}{c} 4.5466 \\ \pm 0.1088 \end{array}$	$\begin{array}{c} 0.6047 \\ \scriptstyle{\pm 0.0169} \end{array}$	$\substack{2.2880 \\ \pm 0.0231}$	$0.9044 \\ \pm 0.0125$	$\begin{array}{c} 0.3923 \\ \scriptstyle{\pm 0.0058} \end{array}$	$0.6554 \\ \pm 0.0132$
	PIG'N'PI	$\begin{array}{c} \textbf{0.0076} \\ \pm 0.0003 \end{array}$	0.0099 ±0.0007	$\begin{array}{c} \textbf{0.0225} \\ \pm \textbf{0.0012} \end{array}$	$\begin{array}{c} \textbf{0.1088} \\ \pm 0.0079 \end{array}$	$\begin{array}{c} \textbf{0.0090} \\ \pm 0.0004 \end{array}$	$\begin{array}{c} \textbf{0.0091} \\ \pm 0.0004 \end{array}$	$\begin{array}{c} \textbf{0.0089} \\ \pm 0.0002 \end{array}$	$\begin{array}{c} \textbf{0.0150} \\ \pm 0.0022 \end{array}$
MAE_{ef}	Baseline	$\begin{array}{c} 1.7644 \\ \scriptstyle{\pm 0.0104} \end{array}$	$\begin{array}{c} 2.4864 \\ \scriptstyle{\pm 0.0104} \end{array}$	$\begin{array}{c} 1.5492 \\ \pm 0.0553 \end{array}$	$\begin{array}{c} 0.5105 \\ \scriptstyle{\pm 0.1459} \end{array}$	$\begin{array}{c} 3.0739 \\ \pm 0.0580 \end{array}$	$\begin{array}{c} 1.9313 \\ \pm 0.0076 \end{array}$	$\begin{array}{c} 0.7243 \\ \scriptstyle{\pm 0.0111} \end{array}$	$1.1630 \\ \scriptstyle{\pm 0.0063}$
:—e	Baseline _{SiLU}	$\substack{2.2647 \\ \pm 0.0420}$	$\substack{2.7155 \\ \pm 0.0333}$	$\substack{2.2720 \\ \pm 0.2375}$	$\begin{array}{c} 1.0911 \\ \scriptstyle{\pm 0.1684} \end{array}$	$\begin{array}{c} 3.4747 \\ \pm 0.0963 \end{array}$	$\begin{array}{c} 2.1853 \\ \pm 0.0321 \end{array}$	$\begin{array}{c} 1.1977 \\ \pm 0.0359 \end{array}$	$\substack{1.6008 \\ \pm 0.0311}$
	PIG'N'PI	$\begin{array}{c} \textbf{0.0023} \\ \pm \textbf{0.0001} \end{array}$	$\begin{array}{c} \textbf{0.0037} \\ \pm \textbf{0.0003} \end{array}$	$\begin{array}{c} \textbf{0.0080} \\ \pm \textbf{0.0006} \end{array}$	$\begin{array}{c} \textbf{0.0223} \\ \pm \textbf{0.0013} \end{array}$	$\begin{array}{c} \textbf{0.0058} \\ \pm \textbf{0.0011} \end{array}$	$\begin{array}{c} \textbf{0.0053} \\ \pm \textbf{0.0005} \end{array}$	0.0016 ±3.4E-5	$\begin{array}{c} \textbf{0.0030} \\ \pm 0.0004 \end{array}$
MAE_{nf}	Baseline	$\begin{array}{c} 8.3353 \\ \pm 0.0627 \end{array}$	13.1721 ±0.0716	$\begin{array}{c} 9.3034 \\ \pm 0.3807 \end{array}$	2.6295 ±0.6315	14.1222 ±0.3045	$\begin{array}{c} 9.1354 \\ \pm 0.0546 \end{array}$	$\substack{4.6927 \\ \pm 0.0584}$	$\begin{array}{c} 6.7873 \\ \scriptstyle{\pm 0.0566} \end{array}$
1417 (E)	Baseline _{SiLU}	10.3496 ±0.1832	14.1069 ±0.1588	10.6447 ±1.0175	5.1109 ±0.6467	16.2250 ±0.5242	10.5310 ±0.1533	$7.9723 \\ \pm 0.2558$	9.6495 ±0.1291
	PIG'N'PI	$\begin{array}{c} \textbf{0.0080} \\ \pm 0.0003 \end{array}$	0.0104 ±0.0007	0.0261 ±0.0014	$\begin{array}{c} \textbf{0.1212} \\ \pm \textbf{0.0085} \end{array}$	$\begin{array}{c} \textbf{0.0115} \\ \pm \textbf{0.0006} \end{array}$	0.0118 ±0.0005	0.0098 ±0.0002	0.0160 ±0.0023
MAE_{\Deltaep}	Baseline	$\begin{array}{c} 0.9588 \\ \pm 0.0048 \end{array}$	$\begin{array}{c} 1.1007 \\ \pm 0.0058 \end{array}$	$\begin{array}{c} 0.4656 \\ \pm 0.0046 \end{array}$	$0.3734 \\ \pm 0.2349$	$\begin{array}{c} 1.3174 \\ \pm 0.0442 \end{array}$	1.1298 ±0.0088	$0.5979 \atop \pm 0.0210$	$0.8568 \\ \pm 0.0167$
ти с—дер	Baseline _{SiLU}	1.2192 ±0.0296	1.2418 ±0.0226	1.6590 ±0.3484	1.3053 ±0.2559	$^{1.4173}_{\pm 0.0648}$	1.1852 ±0.0376	$0.9872 \atop \pm 0.0395$	1.0427 ±0.0415
	PIG'N'PI	0.0005 ±1.4E-5	0.0016 ±0.0003	0.0096 ±0.0009	0.0156 ±0.0015	0.0048 ±0.0017	0.0031 ±0.0006	0.2197 ±0.0001	0.2344 ±0.0001
MAE_{\Deltanp}	Baseline	4.0389 ±0.2410	5.5378 ±0.1083	1.5875 ±0.0363	1.6498 ±1.2898	4.9960 ±0.3848	4.7247 ±0.0448	$\substack{2.9314 \\ \pm 0.2362}$	3.7998 ±0.2532
тит с—дпр	Baseline _{SiLU}	5.3748 ±0.6218	6.0889 ±0.2634	6.3113 ±1.7498	6.2894 ±0.8594	5.4304 ±0.5369	5.1887 ±0.1327	5.2514 ±0.3821	4.9127 ±0.5259
	PIG'N'PI	$\begin{array}{c} \textbf{0.0016} \\ \pm \textbf{0.0001} \end{array}$	$\begin{array}{c} \textbf{0.0062} \\ \pm \textbf{0.0012} \end{array}$	0.0179 ±0.0011	$\begin{array}{c} \textbf{0.0381} \\ \pm 0.0037 \end{array}$	0.0129 ±0.0046	0.0074 ±0.0009	0.9319 ±0.0005	$\begin{array}{c} \textbf{0.9322} \\ \pm 0.0004 \end{array}$
MAE^P_symm	Baseline	$\begin{array}{c} 0.5641 \\ \scriptstyle{\pm 0.0119} \end{array}$	$0.4931 \\ \pm 0.0056$	$\begin{array}{c} 0.1094 \\ \pm 0.0055 \end{array}$	$\begin{array}{c} 0.2663 \\ \scriptstyle{\pm 0.3068} \end{array}$	$0.8017 \\ \pm 0.0528$	$0.4261 \atop \pm 0.0121$	$0.3538 \atop \pm 0.0222$	$0.3474 \\ \pm 0.0106$
www.isymm	Baseline _{SiLU}	1.1668 ±0.0281	0.9798 ±0.0735	1.8888 ±0.6032	1.2961 ±0.3374	1.0689 ±0.0443	0.7108 ±0.0394	$0.8908 \\ \pm 0.0287$	0.8612 ±0.0305
	PIG'N'PI	0.0007 ±0.0001	0.0025 ±0.0008	0.0074 ±0.0010	0.0062 ±0.0005	0.0252 ±0.0065	0.0422 ±0.0144	0.0003 ±2.1E-5	0.0005 ±2.6E-5

A.3 Evaluation of the generalization ability on learning the pairwise force and potential energy

We evaluate the generalization ability of the baseline model, GN+ and PIG'N'PI by first training the models on an eight-particle system and then evaluating their performance on a 12-particle system. We evaluate the performance of baseline model, GN+ and PIG'N'PI on the pairwise force learning task (Table 5) and baseline model and PIG'N'PI on the pairwise potential energy learning task (Table 6) because GN+ is only designed for learning the pairwise force. Furthermore, a limitation of GN+ is, after training, it cannot be generalized to predict the acceleration for a new system. The reason is the learnt node property is specifically associated to the system used for training. We need to train GN+ from scratch again to predict the acceleration for a new system.

Table 5: Evaluation of the generalization ability on the pairwise force learning task. Models are trained on a eight-particle system and then tested on a 12-particle system. Results averaged across five experiments. Note that GN+ cannot be generalized to predict the acceleration because of the learnt node property.

		Spring dim=2	Spring dim=3	Charge dim=2	Charge dim=3	Orbital dim=2	Orbital dim=3	Discnt dim=2	Discnt dim=3
MAE _{acc}	Baseline	$\begin{array}{c} 0.2790 \\ \pm 0.0402 \end{array}$	$\begin{array}{c} 0.5664 \\ \pm 0.0630 \end{array}$	$\begin{array}{c} 1.0363 \\ \pm 0.0780 \end{array}$	$\substack{2.2038 \\ \pm 0.3393}$	$\begin{array}{c} 0.1007 \\ \pm 0.0096 \end{array}$	$\begin{array}{c} 0.1497 \\ \pm 0.0166 \end{array}$	$\begin{array}{c} 0.2067 \\ \scriptstyle{\pm 0.0217} \end{array}$	$\begin{array}{c} 0.3705 \\ \scriptstyle{\pm 0.0274} \end{array}$
400	GN+	-	-	-	-	-	-	-	-
	PIG'N'PI	$\begin{array}{c} \textbf{0.0449} \\ \pm 0.0014 \end{array}$	$\begin{array}{c} \textbf{0.0680} \\ \pm 0.0034 \end{array}$	$\begin{array}{c} \textbf{0.3561} \\ \pm 0.0481 \end{array}$	0.5467 ±0.0441	$\begin{array}{c} \textbf{0.0413} \\ \pm \textbf{0.0020} \end{array}$	$\begin{array}{c} \textbf{0.0407} \\ \pm \textbf{0.0010} \end{array}$	$\begin{array}{c} \textbf{0.0489} \\ \pm \textbf{0.0042} \end{array}$	$\begin{array}{c} \textbf{0.0726} \\ \pm 0.0014 \end{array}$
MAE_{ef}	Baseline	$\substack{2.1514 \\ \pm 0.1950}$	$\begin{array}{c} 4.2343 \\ \pm 0.7791 \end{array}$	$\begin{array}{c} 0.6920 \\ \scriptstyle{\pm 0.0616} \end{array}$	$\begin{array}{c} 0.6283 \\ \scriptstyle{\pm 0.1043} \end{array}$	$\begin{array}{c} 3.3921 \\ \pm 0.1321 \end{array}$	$\begin{array}{c} 3.3837 \\ \pm 0.7063 \end{array}$	$\substack{1.6555 \\ \pm 0.1018}$	$\substack{2.7026 \\ \pm 0.3773}$
···· ·—e	GN+	$0.5563 \\ \pm 0.2231$	$\begin{array}{c} 0.3990 \\ \scriptstyle{\pm 0.3266} \end{array}$	$\begin{array}{c} 0.5907 \\ \scriptstyle{\pm 0.0102} \end{array}$	$\begin{array}{c} 0.3177 \\ \pm 0.0053 \end{array}$	$\begin{array}{c} 0.6381 \\ \scriptstyle{\pm 0.0030} \end{array}$	$\begin{array}{c} 0.5792 \\ \scriptstyle{\pm 0.0328} \end{array}$	$\begin{array}{c} 0.3717 \\ \scriptstyle{\pm 0.2698} \end{array}$	$0.7442 \\ \pm 0.5024$
	PIG'N'PI	$\begin{array}{c} \textbf{0.0087} \\ \pm \textbf{0.0002} \end{array}$	$\begin{array}{c} \textbf{0.0149} \\ \pm \textbf{0.0008} \end{array}$	$\begin{array}{c} \textbf{0.0481} \\ \pm \textbf{0.0065} \end{array}$	$\begin{array}{c} \textbf{0.0697} \\ \pm 0.0043 \end{array}$	$\begin{array}{c} \textbf{0.0111} \\ \pm \textbf{0.0008} \end{array}$	$\begin{array}{c} \textbf{0.0113} \\ \pm \textbf{0.0004} \end{array}$	$\begin{array}{c} \textbf{0.0052} \\ \pm \textbf{0.0005} \end{array}$	$\begin{array}{c} \textbf{0.0092} \\ \pm \textbf{0.0002} \end{array}$
MAE_{nf}	Baseline	14.7789 ±1.4639	$\begin{array}{c} 34.1458 \\ \pm 6.3003 \end{array}$	$\begin{array}{c} 5.8505 \\ \pm 0.5123 \end{array}$	$\begin{array}{c} 5.2545 \\ \pm 1.0215 \end{array}$	$^{21.1451}_{\pm 0.9028}$	$23.0175 \\ \pm 4.7677$	$16.5313 \atop \pm 1.0373$	25.0296 ±3.6511
(=	GN+	$\begin{array}{c} 3.8516 \\ \scriptstyle{\pm 1.5444} \end{array}$	$\begin{array}{c} 3.2087 \\ \scriptstyle{\pm 2.6770} \end{array}$	$\begin{array}{c} 4.9887 \\ \scriptstyle{\pm 0.0858} \end{array}$	$\underset{\pm 0.0388}{2.3699}$	$\begin{array}{c} 4.0284 \\ \pm 0.0148 \end{array}$	$\begin{array}{c} 3.8214 \\ \scriptstyle{\pm 0.2360} \end{array}$	$\begin{array}{c} 3.7130 \\ \scriptstyle{\pm 2.7434} \end{array}$	6.5094 ±4.1421
	PIG'N'PI	$\begin{array}{c} \textbf{0.0443} \\ \pm \textbf{0.0012} \end{array}$	$\begin{array}{c} \textbf{0.0665} \\ \pm \textbf{0.0033} \end{array}$	$\begin{array}{c} \textbf{0.4178} \\ \pm \textbf{0.0614} \end{array}$	$\begin{array}{c} \textbf{0.5564} \\ \pm 0.0425 \end{array}$	$\begin{array}{c} \textbf{0.0476} \\ \pm \textbf{0.0029} \end{array}$	$\begin{array}{c} \textbf{0.0451} \\ \pm \textbf{0.0011} \end{array}$	$\begin{array}{c} \textbf{0.0477} \\ \pm \textbf{0.0039} \end{array}$	$\begin{array}{c} \textbf{0.0730} \\ \pm 0.0016 \end{array}$
MAE^F_symm	Baseline	$^{1.0060}_{\pm 0.0711}$	$\substack{1.6034 \\ \pm 0.0494}$	$\begin{array}{c} 0.1059 \\ \scriptstyle{\pm 0.0158} \end{array}$	$\begin{array}{c} 0.6677 \\ \scriptstyle{\pm 0.2549} \end{array}$	$\begin{array}{c} 1.6018 \\ \pm 0.1370 \end{array}$	$\substack{1.6047 \\ \pm 0.0858}$	$\begin{array}{c} 0.8586 \\ \scriptstyle{\pm 0.0239} \end{array}$	$1.2154 \\ \pm 0.0622$
symm	GN+	$\begin{array}{c} 0.0452 \\ \pm 0.0372 \end{array}$	$\begin{array}{c} 0.0731 \\ \pm 0.0250 \end{array}$	$0.0775 \\ \pm 0.0065$	$\begin{array}{c} 0.0357 \\ \pm 0.0032 \end{array}$	$\begin{array}{c} 0.7903 \\ \scriptstyle{\pm 0.0542} \end{array}$	$\begin{array}{c} 0.7328 \\ \scriptstyle{\pm 0.1140} \end{array}$	$\begin{array}{c} 0.0114 \\ \pm 0.0053 \end{array}$	$0.2427 \atop \pm 0.3709$
	PIG'N'PI	$\begin{array}{c} \textbf{0.0108} \\ \pm \textbf{0.0003} \end{array}$	0.0197 ±0.0008	$\begin{array}{c} \textbf{0.0733} \\ \pm \textbf{0.0125} \end{array}$	$\begin{array}{c} \textbf{0.0614} \\ \pm \textbf{0.0021} \end{array}$	$\begin{array}{c} \textbf{0.0158} \\ \pm 0.0013 \end{array}$	0.0149 ±0.0005	0.0039 ±0.0006	0.0086 ±0.0003

Table 6: Evaluation of the generalization ability on the potential energy learning task. Models are trained on a eight-particle system and then tested on a 12-particle system. Results averaged across five experiments. Here, the comparison model does not contain GN+ because it is only designed for learning force.

		Spring dim=2	Spring dim=3	Charge dim=2	Charge dim=3	Orbital dim=2	Orbital dim=3	Discnt dim=2	Discnt dim=3
MAE _{acc}	Baseline	6.7336 ±0.0626	$14.697 \\ \pm 0.3470$	$\begin{array}{c} 6.2643 \\ \pm 0.7284 \end{array}$	$\begin{array}{c} 3.5436 \\ \pm 0.3228 \end{array}$	5.5236 ±0.0863	$\begin{array}{c} 6.0802 \\ \pm 0.0930 \end{array}$	$\substack{2.6173 \\ \pm 0.1238}$	5.4259 ±0.3450
	PIG'N'PI	$\begin{array}{c} \textbf{0.0180} \\ \pm 0.0018 \end{array}$	$\begin{array}{c} \textbf{0.0238} \\ \pm \textbf{0.0025} \end{array}$	$\begin{array}{c} \textbf{1.1900} \\ \pm \textbf{0.3611} \end{array}$	$\begin{array}{c} \textbf{0.5542} \\ \pm \textbf{0.0644} \end{array}$	$\begin{array}{c} \textbf{0.0760} \\ \pm 0.0167 \end{array}$	$\begin{array}{c} \textbf{0.0995} \\ \pm 0.0198 \end{array}$	$\begin{array}{c} \textbf{0.0215} \\ \pm \textbf{0.0017} \end{array}$	$\begin{array}{c} \textbf{0.0311} \\ \pm \textbf{0.0020} \end{array}$
MAE _{ef}	Baseline	1.7397 ±0.0114	2.6430 ±0.0120	$0.8552 \atop \pm 0.0267$	0.5264 ±0.1457	2.3356 ±0.0487	1.7652 ±0.0116	$0.7328 \\ \pm 0.0148$	1.1855 ±0.0213
	PIG'N'PI	$\begin{array}{c} \textbf{0.0034} \\ \pm \textbf{0.0002} \end{array}$	$\begin{array}{c} \textbf{0.0049} \\ \pm 0.0004 \end{array}$	$\begin{array}{c} \textbf{0.1385} \\ \pm \textbf{0.0357} \end{array}$	$\begin{array}{c} \textbf{0.0631} \\ \pm \textbf{0.0065} \end{array}$	$\begin{array}{c} \textbf{0.0144} \\ \pm \textbf{0.0020} \end{array}$	$\begin{array}{c} \textbf{0.0186} \\ \pm 0.0039 \end{array}$	$\begin{array}{c} \textbf{0.0022} \\ \pm \textbf{0.0001} \end{array}$	$\begin{array}{c} \textbf{0.0040} \\ \pm \textbf{0.0003} \end{array}$
MAE _{nf}	Baseline	11.819 ±0.0599	$\begin{array}{c} 21.083 \\ \scriptstyle{\pm 0.1454} \end{array}$	$7.5812 \atop \pm 0.2963$	$\begin{array}{c} 3.7500 \\ \pm 0.7783 \end{array}$	$15.014 \\ \pm 0.3101$	$^{12.254}_{\pm 0.1030}$	$7.2370 \atop \pm 0.1482$	$^{10.400}_{\scriptstyle{\pm 0.0918}}$
	PIG'N'PI	$\begin{array}{c} \textbf{0.0173} \\ \pm \textbf{0.0013} \end{array}$	$\begin{array}{c} \textbf{0.0233} \\ \pm \textbf{0.0022} \end{array}$	$\begin{array}{c} \textbf{1.3505} \\ \pm \textbf{0.3867} \end{array}$	$\begin{array}{c} \textbf{0.5486} \\ \pm \textbf{0.0646} \end{array}$	$\begin{array}{c} \textbf{0.0704} \\ \pm \textbf{0.0138} \end{array}$	$\begin{array}{c} \textbf{0.0930} \\ \pm 0.0171 \end{array}$	$\begin{array}{c} \textbf{0.0204} \\ \pm \textbf{0.0013} \end{array}$	$\begin{array}{c} \textbf{0.0317} \\ \pm \textbf{0.0022} \end{array}$
MAE_{\Deltaep}	Baseline	$\substack{2.1921 \\ \pm 0.0082}$	$\begin{array}{c} 3.1820 \\ \scriptstyle{\pm 0.0284} \end{array}$	$0.5311 \\ \pm 0.0044$	$\begin{array}{c} 0.4822 \\ \scriptstyle{\pm 0.1159} \end{array}$	$\begin{array}{c} 0.9830 \\ \scriptstyle{\pm 0.0112} \end{array}$	$\begin{array}{c} 0.9161 \\ \scriptstyle{\pm 0.0032} \end{array}$	$\begin{array}{c} 0.7449 \\ \scriptstyle{\pm 0.0165} \end{array}$	$1.7985 \atop \pm 0.0182$
	PIG'N'PI	$\begin{array}{c} \textbf{0.0022} \\ \pm \textbf{0.0002} \end{array}$	$\begin{array}{c} \textbf{0.0033} \\ \pm \textbf{0.0004} \end{array}$	$\begin{array}{c} \textbf{0.0516} \\ \pm 0.0072 \end{array}$	$\begin{array}{c} \textbf{0.0428} \\ \pm \textbf{0.0037} \end{array}$	$\begin{array}{c} \textbf{0.0086} \\ \pm \textbf{0.0007} \end{array}$	$\begin{array}{c} \textbf{0.0106} \\ \pm \textbf{0.0023} \end{array}$	$\begin{array}{c} \textbf{0.2238} \\ \pm \textbf{0.0001} \end{array}$	$\begin{array}{c} \textbf{0.2415} \\ \pm \textbf{0.0003} \end{array}$
MAE_{\Deltanp}	Baseline	$19.256 \atop \pm 0.0530$	$\begin{array}{c} 28.514 \\ \pm 0.4680 \end{array}$	$\begin{array}{c} 2.0988 \\ \scriptstyle{\pm 0.0294} \end{array}$	$1.9149 \\ \pm 1.0773$	$7.1296 \\ \scriptstyle{\pm 0.2341}$	$\begin{array}{c} 7.4346 \\ \pm 0.1342 \end{array}$	5.6309 ±0.2235	$15.478 \atop \pm 0.2467$
	PIG'N'PI	$\begin{array}{c} \textbf{0.0137} \\ \pm \textbf{0.0022} \end{array}$	$\begin{array}{c} \textbf{0.0166} \\ \pm 0.0049 \end{array}$	$\begin{array}{c} \textbf{0.2937} \\ \pm \textbf{0.0485} \end{array}$	$\begin{array}{c} \textbf{0.1668} \\ \pm 0.0173 \end{array}$	$\begin{array}{c} \textbf{0.0415} \\ \pm \textbf{0.0063} \end{array}$	$\begin{array}{c} \textbf{0.0503} \\ \pm \textbf{0.0105} \end{array}$	$\begin{array}{c} \textbf{1.3273} \\ \pm \textbf{0.0009} \end{array}$	$\begin{array}{c} \textbf{1.8850} \\ \pm \textbf{0.0028} \end{array}$
MAE^P_symm	Baseline	$0.4309 \\ \pm 0.0094$	$0.5237 \\ \pm 0.0743$	$0.0481 \\ \pm 0.0048$	$0.2303 \\ \pm 0.2488$	0.6652 ±0.0404	$\begin{array}{c} 0.3765 \\ \scriptstyle{\pm 0.0188} \end{array}$	$0.3753 \\ \pm 0.0190$	0.3894 ±0.0914
-,	PIG'N'PI	0.0010 ±0.0001	0.0033 ±0.0007	0.0159 ±0.0027	0.0124 ±0.0011	0.0219 ±0.0065	0.0336 ±0.0099	0.0004 ±0.0001	0.0009 ±0.0001

A.4 Potential energy prediction in the discontinuous dataset

Here, we take a closer look at the discontinuous dataset as it presented a particularly large MAE $_{\Delta ep}$ for PIG'N'PI predictions compared to the other (continuous) datasets (Fig. 6). The potential energy field P presents a discontinuity at r=2 (see Fig. 10(A)), where P=0 for r<2 and $P\geq0.5$ for $r\geq2$. PIG'N'PI, however, appears to infer a continuous potential function $P_{\text{PIG'N'PI}}$ (see Fig. 10(B)) that presents similar trades to the ground-truth but without the discontinuity. In fact, PIG'N'PI infers the shape of the potential energy function independently in the two areas separated by r=2 without learning the absolute value of the potential energy (see $P_{\text{PIG'N'PI}}-P$ in Fig. 10(C)). The reported mean values of $P_{\text{PIG'N'PI}}-P$ for each area (see Fig. 10(C)) are relatively large indicating the error in the absolute value, whereas the values for the standard deviation are small in both areas showing that PIG'N'PI infers well the shape of the potential (*i.e.*, the derivative of the potential).

Note that the difference in the mean values between the two areas suggests that the absolute value is differently incorrect in the two areas. This explains why the $MAE_{\Delta ep}$ of PIG'N'PI is larger on the discontinuous dataset (Fig. 6) compared to other datasets. Here, PIG'N'PI learns the shape of the potential energy function in two ranges separately, and hence introduces a different discontinuity, which leads to an arbitrary constant that is integrated into the $MAE_{\Delta ep}$ computation over the *entire* space. Therefore, the increased value of $MAE_{\Delta ep}$ simply indicates that the discontinuity in the potential cannot be normalized-out with a measure of the relative potential energy as for the continuous datasets.

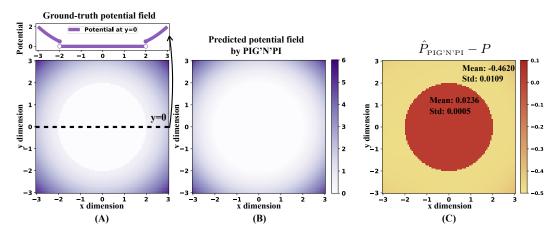


Figure 10: Ground-truth potential energy and predicted potential energy of PIG'N'PI for the Discontinuous dataset. (A) The ground-truth discontinuous potential field around a fixed particle at center. The potential between two particles is discontinuous at distance r=2. (top) Cross-section of the potential at y=0. (B) The predicted potential field by PIG'N'PI. (C) Difference between the potential field predicted by PIG'N'PI and the ground-truth: $\hat{P}_{\text{PIG'N'PI}}-P$. The mean value and standard deviation are computed separately for the two areas limited by the position of the discontinuity in the potential, r=2.

A.5 Performance evaluation for the LJ-argon dataset

Table 7 and Table 8 report the performance of PIG'N'PI to learn pairwise force and pairwise potential energy. $\mathsf{MAE}_{\mathsf{acc}}$, $\mathsf{MAE}_{\mathsf{Aep}}$, $\mathsf{MAE}_{\mathsf{afp}}$, $\mathsf{MAE}_{\mathsf{eff}}$, $\mathsf{MAE}_{\mathsf{nff}}$, $\mathsf{MAE}_{\mathsf{symm}}^F$ and $\mathsf{MAE}_{\mathsf{symm}}^P$ are defined same as before (see Sec. 3.1 and Sec. A.2). We also compute the division between each error and the average of its corresponding ground-truth as the relative error. For example, the relative $\mathsf{MAE}_{\mathsf{acc}} = \mathsf{MAE}_{\mathsf{acc}}/\frac{1}{N}\frac{1}{T}\sum_{i=1}^{N}\sum_{t=1}^{T}|\ddot{r}_i^t|$. Note that the relative $\mathsf{MAE}_{\mathsf{acc}}$ equals to the relative $\mathsf{MAE}_{\mathsf{nf}}$ because all particles have the same mass. Baseline α_{me} refers to the baseline model with symmetry regularization. See Sec. 5.3 for the details of imposing the symmetry regularization into baseline. We can find that symmetry regularization makes the baseline model perform better in terms of $\mathsf{MAE}_{\mathsf{ef}}$. However, PIG'N'PI is still significantly better than the extended baseline. Furthermore, when evaluate the models to learn pairwise force, we also test the method GN+ proposed by [33] to learn pairwise force (see Sec. 5.4). Considering particles in this dataset have the same mass, we also test a variant of GN+ such that we assign all nodes with a unique learnable scalar. We denote this variant as GN+_{uni}. We can see that GN+_{uni} is better than the baseline and GN+. However, PIG'N'PI still outperforms GN+_{uni} by more than one order of magnitude, especially if we look at the $\mathsf{MAE}_{\mathsf{ef}}$ which measures the quality of the predicted pariwise force.

Table 7: Evaluation of the performance to learn pairwise force for the LJ-argon dataset. Results averaged across five experiments.

	MAE _{acc} (Å/ps ²)	Relative MAE _{acc}	MAE _{nf} (meV/Å)	Relative MAE _{nf}	MAE _{ef} (meV/Å)	Relative MAE _{ef}	MAE^F_{symm} $(\mathrm{meV/\mathring{A}})$	Relative MAE_{symm}^{F}
Baseline	0.4230 ±0.0206	2.66% ±0.13%	1.7493 ±0.0850	2.66% ±0.13%	7.2635 ±0.8811	269.41% ±32.68%	0.3885 ±0.0425	14.41% ±1.58%
$Baseline_{\alpha=0.1}$	$\begin{array}{c} 0.6326 \\ \scriptstyle{\pm 0.0381} \end{array}$	$\begin{array}{c} 3.97\% \\ \pm 0.24\% \end{array}$	$\substack{2.6160 \\ \pm 0.1576}$	$\begin{array}{c} 3.97\% \\ \pm 0.24\% \end{array}$	$\begin{array}{c} 3.0155 \\ \pm 0.3660 \end{array}$	$^{111.85\%}_{\scriptstyle{\pm 13.57\%}}$	$\begin{array}{c} 0.1263 \\ \scriptstyle{\pm 0.0050} \end{array}$	4.68% ±0.19%
$Baseline_{\alpha=1}$	$\begin{array}{c} 0.8022 \\ \scriptstyle{\pm 0.0706} \end{array}$	$5.04\% \\ {\scriptstyle \pm 0.44\%}$	$\begin{array}{c} 3.3171 \\ \pm 0.2918 \end{array}$	$5.04\% \\ {\scriptstyle \pm 0.44\%}$	$\substack{2.7034 \\ \pm 0.2164}$	$^{100.27\%}_{\scriptstyle{\pm 8.02\%}}$	$\begin{array}{c} 0.0879 \\ \scriptstyle{\pm 0.0126} \end{array}$	$\begin{array}{c} 3.26\% \\ \scriptstyle{\pm 0.47\%} \end{array}$
Baseline $_{\alpha=10}$	15.1633 ±1.7219	$95.24\% \\ \scriptstyle{\pm 10.81\%}$	$\substack{62.7044 \\ \pm 7.1206}$	$95.24\% \\ \scriptstyle{\pm 10.81\%}$	$\substack{2.6961 \\ \pm 0.0001}$	100.00% ±2.94E-5	$\begin{array}{c} 0.0069 \\ \scriptstyle{\pm 0.0048} \end{array}$	0.26% ±0.18%
Baseline $_{\alpha=100}$	$15.9832 \atop \pm 0.0027$	$^{100.39\%}_{\scriptscriptstyle{\pm 0.02\%}}$	$\substack{66.0951 \\ \pm 0.0110}$	$^{100.39\%}_{\scriptscriptstyle{\pm 0.02\%}}$	$\substack{2.6961 \\ \pm 0.0000}$	$^{100.00\%}_{\scriptscriptstyle{\pm 0.00E0}}$	$\begin{array}{c} \textbf{1.64E-8} \\ \pm \textbf{1.18E-8} \end{array}$	6.07E-9 ±4.37E-9
GN+	15.7991 ±0.0001	99.23% ±3.54E-06	$\substack{65.3337 \\ \pm 0.0002}$	99.23% ±3.54E-06	$\begin{array}{c} 7.7990 \\ \scriptstyle{\pm 0.2822} \end{array}$	$^{289.27\%}_{\scriptstyle{\pm 10.47\%}}$	$\begin{array}{c} 1.1210 \\ \scriptstyle{\pm 0.0599} \end{array}$	41.58% ±2.22%
GN+ _{uni}	$\begin{array}{c} 0.3832 \\ \scriptstyle{\pm 0.1498} \end{array}$	$^{2.41\%}_{_{\pm 0.94\%}}$	$\begin{array}{c} 1.5848 \\ \pm 0.6196 \end{array}$	$^{2.41\%}_{_{\pm 0.94\%}}$	$\begin{array}{c} 0.5799 \\ \pm 0.3035 \end{array}$	$21.51\% \\ \scriptstyle{\pm 11.26\%}$	$\begin{array}{c} 0.0155 \\ \scriptstyle{\pm 0.0092} \end{array}$	0.58% ±0.34%
PIG'N'PI	$\begin{array}{c} \textbf{0.0600} \\ \pm \textbf{0.0020} \end{array}$	$\begin{array}{c} \textbf{0.38\%} \\ \pm \textbf{0.01\%} \end{array}$	$\begin{array}{c} \textbf{0.2483} \\ \pm \textbf{0.0081} \end{array}$	$\begin{array}{c} \textbf{0.38\%} \\ \pm \textbf{0.01\%} \end{array}$	$\begin{array}{c} \textbf{0.0194} \\ \pm \textbf{0.0006} \end{array}$	$0.72\% \\ _{\pm 0.02\%}$	$\begin{array}{c} 0.0270 \\ \scriptstyle{\pm 0.0008} \end{array}$	$1.00\% \\ {\scriptstyle \pm 0.03\%}$

Table 8: Evaluation of the performance to learn pairwise potential energy for the LJ-argon dataset. Results averaged across five experiments.

	MAE _{acc} (Å/ps ²)	Relative MAE _{acc}	MAE _{nf} (meV/Å)	Relative MAE _{nf}	MAE _{ef} (meV/Å)	Relative MAE _{ef}	MAE _{ep} (meV)	Relative MAE _{ep}	$\begin{array}{c} MAE_{np} \\ (meV) \end{array}$	Relative MAE _{np}	MAE^P_{symm} (meV)	Relative MAE ^P _{symm}
Baseline	$^{10.8064}_{\scriptstyle{\pm 0.0113}}$	67.87% ±0.07%	$\begin{array}{c} 44.6875 \\ \pm 0.0467 \end{array}$	67.87% ±0.07%	$73.4575 \atop \pm 6.3486$	2725% ±236%	$13.9532 \atop \pm 1.1882$	1051% ±89.47%	403.866 ±34.9743	510% ±44.2%	21.6873 ±1.8809	1633% ±141.6%
PIG'N'PI	$\begin{array}{c} \textbf{0.0714} \\ \pm \textbf{0.0057} \end{array}$	$0.45\%_{\pm 0.04\%}$	$\begin{array}{c} \textbf{0.2951} \\ \pm \textbf{0.0238} \end{array}$	$0.45\%_{\pm 0.04\%}$	$\begin{array}{c} \textbf{0.0217} \\ \pm \textbf{0.0016} \end{array}$	$0.81\% \\ {\scriptstyle \pm 0.06\%}$	$\begin{array}{c} \textbf{0.0176} \\ \pm \textbf{0.0014} \end{array}$	$1.33\%_{\pm 0.11\%}$	$\begin{array}{c} \textbf{0.4428} \\ \pm \textbf{0.1061} \end{array}$	$0.56\%_{\pm 0.13\%}$	$\begin{array}{c} \textbf{0.0174} \\ \pm \textbf{0.0020} \end{array}$	$1.31\% \\ _{\pm 0.15\%}$

A.6 Evaluation of PIG'N'PI with different activation functions to learn force

Table 9 reports the performance of PIG'N'PI with different activation functions to learn pairwise force.

Table 9: Quality of pairwise force prediction of PIG'N'PI with different activation functions. Results averaged across five experiments.

	-								
		Spring dim=2	Spring dim=3	Charge dim=2	Charge dim=3	Orbital dim=2	Orbital dim=3	Discnt dim=2	Discnt dim=3
	SiLU	0.0206 ±0.0009	0.0278 ±0.0021	0.0425 ±0.0053	0.1191 ±0.0027	0.0202 ±0.0003	0.0182 ±0.0003	0.0227 ±0.0019	0.039 ±0.001
MAE_{acc}	ReLU	0.0339 ±0.0007	0.0524 ±0.0009	0.1528 ±0.0039	0.2058 ±0.0066	0.0402 ±0.0028	0.0399 ±0.0003	0.0463 ±0.0020	0.086 ±0.002
	GELU	0.0171 ±0.0009	0.0189 ±0.0007	0.0401 ±0.0017	0.1247 ±0.0077	0.0212 ±0.0008	0.0191 ±0.0004	0.0232 ±0.0030	0.038 ±0.001
	tanh	0.0234 ±0.0004	0.0645 ±0.0003	0.1713 ±0.0388	0.3252 ±0.0267	0.0415 ±0.0002	0.0860 ±0.0015	0.0646 ±0.0148	0.104 ±0.000
	sigmoid	0.0597 ±0.0046	0.1618 ±0.0173	1.1555 ±0.0121	0.2747 ±0.0455	0.0381 ±0.0042	0.0421 ±0.0024	0.1053 ±0.0014	0.258 ±0.023
	softplus	0.0228 ±0.0011	0.0354 ±0.0018	0.0647 ±0.0071	0.0933 ±0.0045	0.0293 ±0.0018	0.0302 ±0.0012	0.0508 ±0.0017	0.172 ±0.014
	LeakyReLU	0.0326 ±0.0009	0.0545 ±0.0016	0.1477 ±0.0036	0.2212 ±0.0059	0.0387 ±0.0018	0.0396 ±0.0005	0.0494 ±0.0014	0.091 ±0.003
	SiLU	0.0063 ±0.0002	0.0101 ±0.0007	0.0136 ±0.0023	0.0363 ±0.0015	0.0093 ±0.0002	0.0095 ±0.0001	0.0040 ±0.0004	0.007 ±0.000
MAE_{ef}	ReLU	0.0146 ±0.0004	0.0247 ±0.0006	0.0379 ±0.0013	0.0574 ±0.0022	0.0179 ±0.0012	0.0201 ±0.0004	0.0088 ±0.0003	0.020 ±0.000
61	GELU	0.0059 ±0.0003	0.0079 ±0.0003	0.0120 ±0.0005	0.0347 ±0.0020	0.0097 ±0.0004	0.0108 ±0.0003	0.0041 ±0.0006	0.007 ±0.000
	tanh	0.0096 ±0.0003	0.0279 ±0.0002	0.0363 ±0.0068	0.0920 ±0.0075	0.0171 ±0.0003	0.0350 ±0.0007	0.0137 ±0.0033	0.025 ±0.000
	sigmoid	0.0166 ±0.0014	0.0477 ±0.0040	0.2129 ±0.0020	0.0607 ±0.0079	0.0160 ±0.0018	0.0172 ±0.0011	0.0211 ±0.0003	0.065 ±0.007
	softplus	0.0067 ±0.0002	0.0118 ±0.0005	0.0181 ±0.0021	0.0257 ±0.0011	0.0121 ±0.0006	0.0141 ±0.0003	0.0098 ±0.0004	0.036 ±0.002
	LeakyReLU	0.0139 ±0.0006	0.0258 ±0.0011	0.0352 ±0.0008	0.0578 ±0.0023	0.0170 ±0.0009	0.0197 ±0.0006	0.0096 ±0.0004	0.021 ±0.000
	SiLU	0.0219 ±0.0010	0.0292 ±0.0022	0.0488 ±0.0059	0.1317 ±0.0033	0.0260 ±0.0005	0.0233 ±0.0004	0.0239 ±0.0020	0.041 ±0.001
MAE_{nf}	ReLU	0.0358 ±0.0007	0.0552 ±0.0009	0.1694 ±0.0046	0.2246 ±0.0070	0.0483 ±0.0033	0.0494 ±0.0004	0.0489 ±0.0019	0.091 ±0.002
•••	GELU	0.0182 ±0.0009	0.0202 ±0.0007	0.0460 ±0.0017	0.1366 ±0.0078	0.0270 ±0.0010	0.0249 ±0.0006	0.0244 ±0.0032	0.040 ±0.001
	tanh	0.0249 ±0.0006	0.0682 ±0.0003	0.1975 ±0.0444	0.3719 ±0.0303	0.0510 ±0.0003	0.1166 ±0.0018	0.0682 ±0.0157	0.109 ±0.000
	sigmoid	0.0629 ±0.0048	0.1673 ±0.0179	1.3848 ±0.0148	0.3233 ±0.0533	0.0496 ±0.0054	0.0553 ±0.0038	0.1111 ±0.0014	0.272 ±0.024
	softplus	0.0239 ±0.0012	0.0367 ±0.0018	0.0753 ±0.0086	0.1038 ±0.0051	0.0366 ±0.0016	0.0390 ±0.0013	0.0541 ±0.0018	0.182 ±0.016
	LeakyReLU	0.0344 ±0.0010	0.0573 ±0.0018	0.1634 ±0.0044	0.2411 ±0.0058	0.0464 ±0.0022	0.0489 ±0.0005	0.0520 ±0.0016	0.095 ±0.003
	SiLU	0.0075 ±0.0003	0.0133 ±0.0008	0.0185 ±0.0036	0.0345 ±0.0017	0.0136 ±0.0004	0.0134 ±0.0004	0.0026 ±0.0004	0.006 ±0.000
MAE^F_symm	ReLU	0.0205 ±0.0006	0.0350 ±0.0009	0.0459 ±0.0013	0.0477 ±0.0018	0.0256 ±0.0016	0.0285 ±0.0007	0.0104 ±0.0004	0.024 ±0.000
Syllill	GELU	0.0074 ±0.0003	0.0108 ±0.0003	0.0151 ±0.0007	0.0311 ±0.0013	0.0138 ±0.0006	0.0155 ±0.0005	0.0031 ±0.0003	0.007 ±0.000
	tanh	0.0128 ±0.0005	0.0367 ±0.0002	0.0242 ±0.0013	0.0580 ±0.0121	0.0223 ±0.0003	0.0363 ±0.0008	0.0106 ±0.0018	0.026 ±0.000
	sigmoid	0.0108 ±0.0006	0.0337 ±0.0018	0.0386 ±0.0055	0.0344 ±0.0013	0.0194 ±0.0026	0.0193 ±0.0016	0.0094 ±0.0004	0.031 ±0.005
	softplus	0.0072 ±0.0003	0.0145 ±0.0007	0.0217 ±0.0021	0.0252 ±0.0014	0.0163 ±0.0003	0.0195 ±0.0004	0.0068 ±0.0008	0.040 ±0.005
	LeakyReLU	0.0194 ±0.0008	0.0363 ±0.0016	0.0463 ±0.0014	0.0494 ±0.0026	0.0242 ±0.0013	0.0279 ±0.0008	0.0109 ±0.0004	0.025 ±0.000

A.7 Performance evaluation of PIG'N'PI with different activation functions for pairwise potential energy prediction

Table 10 reports the performance of PIG'N'PI with different activation functions to learn pairwise potential energy.

Table 10: Performance evaluation of PIG'N'PI with different activation functions for pairwise potential energy prediction. Results averaged across five experiments.

		Spring	Spring	Charge	Charge	Orbital	Orbital	Discnt	Discnt
		dim=2	dim=3	dim=2	dim=3	dim=2	dim=3	dim=2	dim=3
		0.0076	0.0099	0.0225	0.1088	0.0090	0.0091	0.0089	0.0150
	SiLU	±0.0003	±0.0099	± 0.0012	±0.0079	±0.0004	±0.0004	±0.0002	± 0.0022
		3.2521	5.0524	6.2996					
	ReLU	± 0.0818	±0.0796	±0.0043	1.8127 ± 0.0017	5.6495 ± 0.0788	3.8274 ± 0.0224	1.5069 ± 0.0501	2.8083 ± 0.0224
		0.0063					0.0098	0.0104	0.015
	GELU	±0.0004	0.0054 ± 0.0003	0.0298 ± 0.0010	0.1586 ± 0.0061	0.0089 ± 0.0001	±0.0004	±0.0009	±0.000
MAE_{acc}									
www.acc	tanh	0.0223 ± 0.0023	0.0366	0.0499	0.1949	0.0139	0.0187 ± 0.0006	0.0330	0.088
			±0.0054	±0.0016	±0.0112	±0.0001		±0.0010	±0.010
	sigmoid	0.0949	0.0432	0.0631	0.1022	0.0206	0.0290	0.0299	0.063
		±0.0915	±0.0038	±0.0029	±0.0092	±0.0012	±0.0015	±0.0014	±0.002
	softplus	0.0259	0.0271	0.0516	0.0870	0.0113	0.0161	0.0274	0.043
	•	±0.0029	±0.0019	±0.0034	±0.0049	±0.0005	±0.0018	±0.0023	±0.002
	LeakyReLU	3.3248	5.0494	6.2987	1.8135	5.6056	3.8106	1.5031	2.777
		±0.0626	±0.0265	±0.0070	±0.0017	±0.0270	± 0.0647	±0.0369	±0.040
	SiLU	0.0023	0.0037	0.0080	0.0223	0.0058	0.0053	0.0016	0.003
	-	±0.0001	±0.0003	±0.0006	±0.0013	±0.0011	±0.0005	±3.4E-5	±0.000
	ReLU	1.1132	1.5625	1.2551	0.3854	1.9323	1.3612	0.5471	0.950
		±0.0243	±0.0287	±0.0027	±0.0007	±0.0265	±0.0129	±0.0178	±0.006
	GELU	0.0020	0.0029	0.0114	0.0312	0.0054	0.0062	0.0019	0.003
	-	±0.0001	± 0.0007	± 0.0001	±0.0016	±0.0008	± 0.0004	±0.0002	±0.000
MAE_{ef}	tanh	0.0081	0.0136	0.0214	0.0719	0.0109	0.0150	0.0069	0.022
		±0.0011	± 0.0014	± 0.0006	± 0.0016	± 0.0015	± 0.0011	± 0.0002	± 0.002
	sigmoid	0.0267	0.0123	0.0210	0.0292	0.0113	0.0139	0.0058	0.014
	signioid	±0.0290	± 0.0010	± 0.0013	± 0.0026	± 0.0007	±0.0009	± 0.0003	± 0.000
	softplus	0.0068	0.0103	0.0202	0.0260	0.0073	0.0084	0.0054	0.009
	sortpius	± 0.0007	± 0.0009	± 0.0023	± 0.0022	± 0.0012	± 0.0009	± 0.0005	± 0.000
	LeakyReLU	1.1325	1.5550	1.2511	0.3857	1.9077	1.3596	0.5444	0.942
	LeakyReLU	± 0.0143	± 0.0120	± 0.0026	± 0.0011	± 0.0125	± 0.0250	± 0.0174	± 0.011
	SiLU	0.0080	0.0104	0.0261	0.1212	0.0115	0.0118	0.0098	0.016
	SILU	± 0.0003	± 0.0007	± 0.0014	± 0.0085	± 0.0006	± 0.0005	± 0.0002	± 0.002
	D.III	3.3210	5.1395	7.1663	1.9481	7.2113	4.9279	1.5787	2.895
	ReLU	± 0.0732	± 0.0846	± 0.0054	± 0.0020	± 0.0851	± 0.0347	± 0.0533	± 0.019
	CELL	0.0067	0.0059	0.0347	0.1757	0.0114	0.0128	0.0111	0.016
	GELU	± 0.0005	± 0.0003	± 0.0011	± 0.0071	± 0.0003	± 0.0006	±0.0009	±0.000
MAE_{nf}		0.0235	0.0392	0.0578	0.2202	0.0176	0.0236	0.0355	0.094
	tanh	±0.0023	±0.0056	±0.0018	±0.0131	±0.0003	±0.0007	±0.0010	±0.011
		0.0993	0.0447	0.0738	0.1137	0.0268	0.0369	0.0320	0.067
	sigmoid	± 0.0957	±0.0038	± 0.0034	±0.0095	±0.0016	± 0.0017	± 0.0015	±0.002
		0.0268	0.0283	0.0599	0.0964	0.0148	0.0206	0.0292	0.045
	softplus	± 0.0030	± 0.0019	±0.0037	± 0.0059	±0.0006	± 0.0019	± 0.0023	± 0.002
		3.3932	5.1328	7.1647	1.9487	7.1476	4.8920	1.5798	2.873
	LeakyReLU	±0.0640	± 0.0205	±0.0082	±0.0022	±0.0364	±0.0795	±0.0339	± 0.038
			0.0203	0.0062	⊥0.0022	⊥0.0504		nued on ne	

Continued: Performance evaluation of PIG'N'PI with different activation functions for pairwise potential energy prediction..

	SiLU	0.0005	0.0016	0.0096	0.0156	0.0048	0.0031	0.2197	0.2344
	SILU	±1.4E-5	± 0.0003	± 0.0009	± 0.0015	± 0.0017	± 0.0006	± 0.0001	± 0.0001
	ReLU	1.8798	5.8125	0.4592	0.2061	1.3700	1.0480	0.6844	1.4246
	KCLU	±0.2632	±0.2222	±0.0115	± 0.0042	± 0.1386	± 0.0589	± 0.0786	±0.1339
	GELU	0.0006	0.0017	0.0145	0.0156	0.0034	0.0037	0.2197	0.2344
	GELU	± 0.0001	± 0.0007	± 0.0007	± 0.0020	± 0.0011	± 0.0006	± 0.0001	± 0.0001
MAE_{\Deltaep}	tanh	0.0030	0.0037	0.0312	0.0803	0.0080	0.0102	0.2202	0.2353
	tallii	± 0.0013	± 0.0008	± 0.0008	± 0.0040	± 0.0019	± 0.0010	± 0.0001	± 0.0002
	sigmoid	0.0068	0.0025	0.0271	0.0298	0.0068	0.0074	0.2199	0.2349
	sigmoid	± 0.0094	± 0.0002	± 0.0033	± 0.0048	± 0.0012	± 0.0014	± 0.0002	± 0.0005
	aoftmlus	0.0015	0.0080	0.0315	0.0369	0.0079	0.0065	0.2199	0.2349
	softplus	± 0.0005	± 0.0016	± 0.0059	± 0.0041	± 0.0016	± 0.0013	± 0.0001	± 0.0002
	LookyDalli	2.0263	5.2505	0.4646	0.2081	1.5073	1.1100	0.7408	1.3386
	LeakyReLU	± 0.3663	± 0.6543	± 0.0083	± 0.0034	± 0.1474	± 0.0630	± 0.1149	± 0.1336
	CHII	0.0016	0.0062	0.0179	0.0381	0.0129	0.0074	0.9319	0.9322
	SiLU	± 0.0001	± 0.0012	± 0.0011	± 0.0037	± 0.0046	± 0.0009	± 0.0005	± 0.0004
	Dalii	8.6263	22.7924	1.5514	0.6727	5.3176	4.0300	3.2903	6.6232
	ReLU	± 1.4047	± 2.6079	± 0.0545	± 0.0154	± 1.0821	± 0.2800	± 0.4927	± 1.1136
	GELU	0.0015	0.0044	0.0263	0.0441	0.0085	0.0099	0.9322	0.9319
	GELU	± 0.0002	± 0.0020	± 0.0013	± 0.0053	± 0.0026	± 0.0020	± 0.0003	± 0.0002
MAE_{\Deltanp}	tomb	0.0068	0.0097	0.0469	0.1859	0.0173	0.0234	0.9338	0.9338
	tanh	± 0.0016	± 0.0009	± 0.0023	± 0.0073	± 0.0019	± 0.0029	± 0.0009	± 0.0014
	sigmoid	0.0220	0.0076	0.0398	0.0689	0.0203	0.0211	0.9324	0.9331
		± 0.0312	± 0.0007	± 0.0040	± 0.0111	± 0.0044	± 0.0024	± 0.0011	± 0.0017
	ft1	0.0051	0.0339	0.0463	0.0794	0.0331	0.0307	0.9323	0.9330
	softplus	± 0.0017	± 0.0095	± 0.0069	± 0.0108	± 0.0107	± 0.0097	± 0.0005	± 0.0012
	L anlay Dal II	10.3190	22.1011	1.5917	0.6743	6.1927	4.2487	3.4278	6.1117
	LeakyReLU	±2.5713	± 4.2016	± 0.0667	± 0.0250	± 1.0489	± 0.3877	± 1.0505	± 1.1812
	CHIL	0.0007	0.0025	0.0074	0.0062	0.0252	0.0422	0.0003	0.0005
	SiLU	± 0.0001	± 0.0008	± 0.0010	± 0.0005	± 0.0065	± 0.0144	±2.1E-5	±2.6E-5
	Dat II	1.8823	3.6725	0.1467	0.0702	0.9496	0.7473	0.5693	1.1960
	ReLU	±0.4517	± 0.8805	±0.0339	± 0.0076	± 0.0576	±0.0270	±0.1220	±0.2500
	CELLI	0.0009	0.0047	0.0090	0.0078	0.0521	0.0460	0.0004	0.0008
_	GELU	±0.0005	± 0.0022	± 0.0005	± 0.0009	±0.0149	±0.0176	± 0.0000	±0.0000
MAE^P_symm	4. 1	0.0202	0.0056	0.0155	0.0215	0.1968	0.1172	0.0010	0.0024
-,	tanh	± 0.0327	± 0.0022	±0.0019	± 0.0007	± 0.0592	± 0.0242	± 0.0001	± 0.0001
		0.0059	0.0028	0.0237	0.0130	0.0294	0.0751	0.0006	0.0017
	sigmoid	± 0.0076	± 0.0003	± 0.0071	± 0.0010	±0.0127	± 0.0181	± 0.0000	± 0.0001
	C. 1	0.0017	0.0112	0.0151	0.0115	0.0481	0.0328	0.0007	0.0015
	softplus	±0.0007	± 0.0041	± 0.0070	±0.0012	±0.0427	± 0.0257	±0.0001	± 0.0001
	T 1 D TT	2.1660	3.2254	0.1492	0.0688	0.9544	0.7962	0.5670	0.9258
	LeakyReLU	±0.5849	±1.0211	±0.0203	± 0.0052	±0.0521	±0.0972	±0.2456	±0.1685
									The and

(The end)

A.8 Imposing symmetry regularization on the baseline model to learn force

Table 11 reports the performance of the baseline model with symmetry regularization (see the discussion in Sec. 3.5 and Sec. 5.3). Results show that such symmetry regularization improves the performance of the baseline model with respect to $\mathsf{MAE}^F_{\mathsf{symm}}$, which was expected since the symmetry term was minimized. Furthermore, the symmetry regularization makes the baseline model perform better in terms of $\mathsf{MAE}_{\mathsf{acc}}$, $\mathsf{MAE}_{\mathsf{ef}}$ and $\mathsf{MAE}_{\mathsf{nf}}$ on several datasets. However, PIG'N'PI still significantly outperforms the extended baseline in terms of $\mathsf{MAE}_{\mathsf{acc}}$, $\mathsf{MAE}_{\mathsf{ef}}$ and $\mathsf{MAE}_{\mathsf{nf}}$, which are the most relevant performance evaluation metrics for physics-consistent particle interactions.

Table 11: Comparison of pairwise force prediction of the baseline model, extended baseline model with symmetry regularization with different weights and PIG'N'PI. Results averaged across five experiments.

		Spring dim=2	Spring dim=3	Charge dim=2	Charge dim=3	Orbital dim=2	Orbital dim=3	Discnt dim=2	Discnt dim=3
	Baseline	$0.0565 \\ \pm 0.0023$	$0.1076 \\ \pm 0.0012$	$0.2521 \\ \pm 0.0173$	$0.3824 \\ \pm 0.0559$	$0.0437 \\ \pm 0.0026$	$0.0439 \atop \pm 0.0014$	$0.0592 \\ \pm 0.0015$	$\begin{array}{c} 0.1171 \\ \pm 0.0010 \end{array}$
MAE_{acc}	$\alpha = 0.1$	$0.0756 \\ \pm 0.0015$	$\begin{array}{c} 0.1390 \\ \scriptstyle{\pm 0.0019} \end{array}$	$\begin{array}{c} 0.2611 \\ \scriptstyle{\pm 0.0279} \end{array}$	$\begin{array}{c} 0.2864 \\ \scriptstyle{\pm 0.0117} \end{array}$	$\begin{array}{c} 0.0544 \\ \scriptstyle{\pm 0.0017} \end{array}$	$\begin{array}{c} 0.0567 \\ \scriptstyle{\pm 0.0007} \end{array}$	$\begin{array}{c} 0.0623 \\ \scriptstyle{\pm 0.0016} \end{array}$	$\begin{array}{c} 0.1256 \\ \pm 0.0020 \end{array}$
	$\alpha = 1.0$	$0.0743 \\ \pm 0.0026$	$\begin{array}{c} 0.1465 \\ \scriptstyle{\pm 0.0013} \end{array}$	$\begin{array}{c} 0.2431 \\ \scriptstyle{\pm 0.0092} \end{array}$	$\begin{array}{c} 0.3121 \\ \scriptstyle{\pm 0.0436} \end{array}$	$\begin{array}{c} 0.0799 \\ \scriptstyle{\pm 0.0022} \end{array}$	$\begin{array}{c} 0.0769 \\ \scriptstyle{\pm 0.0014} \end{array}$	$\begin{array}{c} 0.0571 \\ \scriptstyle{\pm 0.0027} \end{array}$	$\begin{array}{c} 0.1135 \\ \pm 0.0026 \end{array}$
	$\alpha = 10$	$0.0676 \\ \pm 0.0012$	$\begin{array}{c} 0.1214 \\ \scriptstyle{\pm 0.0018} \end{array}$	$\begin{array}{c} 5.4372 \\ \pm 0.1597 \end{array}$	$\begin{array}{c} 0.7785 \\ \scriptstyle{\pm 0.0027} \end{array}$	$\begin{array}{c} 0.0769 \\ \scriptstyle{\pm 0.0037} \end{array}$	$\begin{array}{c} 0.0740 \\ \scriptstyle{\pm 0.0012} \end{array}$	$0.0538 \atop \pm 0.0019$	$\begin{array}{c} 0.1017 \\ \pm 0.0039 \end{array}$
	$\alpha = 100$	$0.0770 \\ \pm 0.0027$	$\begin{array}{c} 0.1381 \\ \scriptstyle{\pm 0.0024} \end{array}$	$\begin{array}{c} 5.5282 \\ \pm 0.0249 \end{array}$	$\begin{array}{c} 0.7758 \\ \scriptstyle{\pm 0.0042} \end{array}$	$\begin{array}{c} 0.0902 \\ \scriptstyle{\pm 0.0013} \end{array}$	$\begin{array}{c} 0.1068 \\ \scriptstyle{\pm 0.0028} \end{array}$	$\begin{array}{c} 0.0573 \\ \scriptstyle{\pm 0.0022} \end{array}$	$\begin{array}{c} 0.1064 \\ \scriptstyle{\pm 0.0017} \end{array}$
	PIG'N'PI	$\begin{array}{c} \textbf{0.0206} \\ \pm \textbf{0.0009} \end{array}$	$\begin{array}{c} \textbf{0.0278} \\ \pm \textbf{0.0021} \end{array}$	$\begin{array}{c} \textbf{0.0425} \\ \pm \textbf{0.0053} \end{array}$	$\begin{array}{c} \textbf{0.1191} \\ \pm \textbf{0.0027} \end{array}$	$\begin{array}{c} \textbf{0.0202} \\ \pm \textbf{0.0003} \end{array}$	$\begin{array}{c} \textbf{0.0182} \\ \pm \textbf{0.0003} \end{array}$	$\begin{array}{c} \textbf{0.0227} \\ \pm \textbf{0.0019} \end{array}$	$\begin{array}{c} \textbf{0.0399} \\ \pm 0.0011 \end{array}$
	Baseline	2.3979 ±0.2095	3.8952 ±0.7178	1.1832 ±0.0955	0.6447 ±0.1118	4.1010 ±0.1467	3.5379 ±0.7571	1.6536 ±0.0640	2.5803 ±0.2886
MAE_{ef}	$\alpha = 0.1$	1.6465 ±0.1523	2.6250 ±0.1347	1.2490 ±0.1001	$0.3751 \\ \pm 0.0167$	2.4493 ±0.1253	1.7196 ±0.1193	0.5302 ±0.0191	1.2120 ±0.0456
	$\alpha = 1.0$	1.5304 ±0.1035	$\underset{\pm 0.0925}{2.4136}$	$^{1.2811}_{\pm 0.0343}$	$0.3754 \\ \pm 0.0043$	$\substack{2.3558 \\ \pm 0.1536}$	$\substack{1.7502 \\ \pm 0.0739}$	$\begin{array}{c} 0.5250 \\ \scriptstyle{\pm 0.0861} \end{array}$	$0.9572 \\ \pm 0.0394$
	$\alpha = 10$	$\begin{array}{c} 1.6178 \\ \scriptstyle{\pm 0.0424} \end{array}$	$\begin{array}{c} 2.3723 \\ \scriptstyle{\pm 0.0327} \end{array}$	$\substack{1.2531 \\ \pm 0.0004}$	0.3790 ±1E-11	$\substack{2.3495 \\ \pm 0.0267}$	$^{1.7543}_{\pm 0.0317}$	$\begin{array}{c} 0.4819 \\ \scriptstyle{\pm 0.0125} \end{array}$	$\begin{array}{c} 0.9746 \\ \scriptstyle{\pm 0.0191} \end{array}$
	$\alpha = 100$	$1.5694 \\ \pm 0.0167$	$\substack{2.3943 \\ \pm 0.0078}$	1.2528 ±2E-11	0.3790 ±9E-12	$\underset{\pm 0.0077}{2.3632}$	$\substack{1.7505 \\ \pm 0.0066}$	$\begin{array}{c} 0.4893 \\ \scriptstyle{\pm 0.0053} \end{array}$	$\begin{array}{c} 0.9796 \\ \scriptstyle{\pm 0.0056} \end{array}$
	PIG'N'PI	$\begin{array}{c} \textbf{0.0063} \\ \pm \textbf{0.0002} \end{array}$	$\begin{array}{c} \textbf{0.0101} \\ \pm \textbf{0.0007} \end{array}$	$\begin{array}{c} \textbf{0.0136} \\ \pm \textbf{0.0023} \end{array}$	$\begin{array}{c} \textbf{0.0363} \\ \pm \textbf{0.0015} \end{array}$	$\begin{array}{c} \textbf{0.0093} \\ \pm \textbf{0.0002} \end{array}$	$\begin{array}{c} \textbf{0.0095} \\ \pm \textbf{0.0001} \end{array}$	$\begin{array}{c} \textbf{0.0040} \\ \pm \textbf{0.0004} \end{array}$	$\begin{array}{c} \textbf{0.0079} \\ \pm \textbf{0.0002} \end{array}$
	Baseline	$11.652 \\ \pm 0.9890$	$20.967 \\ \pm 3.8552$	$\begin{array}{c} 6.831 \\ \scriptstyle{\pm 0.5548} \end{array}$	$\begin{array}{c} 3.804 \\ \scriptstyle{\pm 0.7523} \end{array}$	$18.194 \atop \pm 0.6884$	$16.677 \\ \pm 3.5212$	$10.786 \atop \pm 0.3764$	$15.651 \atop \pm 1.7983$
MAE_{nf}	$\alpha = 0.1$	$\begin{array}{c} 7.9466 \\ \scriptstyle{\pm 0.7318} \end{array}$	$\begin{array}{c} 14.104 \\ \scriptstyle{\pm 0.7268} \end{array}$	$\begin{array}{c} 7.2125 \\ \scriptstyle{\pm 0.5854} \end{array}$	$\begin{array}{c} 1.9825 \\ \scriptstyle{\pm 0.0927} \end{array}$	$10.675 \atop \pm 0.5594$	$\begin{array}{c} 7.9656 \\ \pm 0.5602 \end{array}$	$\begin{array}{c} 3.4844 \\ \scriptstyle{\pm 0.1278} \end{array}$	$\begin{array}{c} 7.4980 \\ \pm 0.2871 \end{array}$
	$\alpha = 1.0$	$7.3867 \atop \pm 0.5031$	$12.954 \\ \pm 0.4993$	$7.3978 \atop \pm 0.2000$	$\substack{1.9827 \\ \pm 0.0248}$	$10.257 \atop \scriptstyle{\pm 0.6695}$	$\begin{array}{c} 8.1068 \\ \pm 0.3377 \end{array}$	$\substack{3.4632 \\ \pm 0.5716}$	$\begin{array}{c} 5.9257 \\ \pm 0.2496 \end{array}$
	$\alpha = 10$	$7.8101 \atop \pm 0.2030$	$\begin{array}{c} 12.734 \\ \scriptstyle{\pm 0.1777} \end{array}$	$\begin{array}{c} 7.2335 \\ \pm 0.0002 \end{array}$	$\underset{\pm 4.4\text{E-8}}{2.0040}$	$\begin{array}{c} 10.228 \\ \scriptstyle{\pm 0.1156} \end{array}$	$\begin{array}{c} 8.1252 \\ \pm 0.1463 \end{array}$	$\begin{array}{c} 3.1834 \\ \scriptstyle{\pm 0.0838} \end{array}$	$\begin{array}{c} 6.0471 \\ \scriptstyle{\pm 0.1201} \end{array}$
	$\alpha = 100$	$7.5755 \\ \pm 0.0808$	$12.851 \atop \scriptstyle{\pm 0.0429}$	$\begin{array}{c} 7.2335 \\ \scriptstyle{\pm 1.3\text{E-7}} \end{array}$	2.0040 ±2.5E-8	$10.289 \\ \scriptstyle{\pm 0.0334}$	$\begin{array}{c} 8.1077 \\ \scriptstyle{\pm 0.0307} \end{array}$	$\begin{array}{c} 3.2333 \\ \scriptstyle{\pm 0.0349} \end{array}$	$\begin{array}{c} 6.0803 \\ \pm 0.0346 \end{array}$
	PIG'N'PI	$\begin{array}{c} \textbf{0.0219} \\ \pm \textbf{0.0010} \end{array}$	$\begin{array}{c} \textbf{0.0292} \\ \pm \textbf{0.0022} \end{array}$	$\begin{array}{c} \textbf{0.0488} \\ \pm \textbf{0.0059} \end{array}$	$\begin{array}{c} \textbf{0.1317} \\ \pm \textbf{0.0033} \end{array}$	$\begin{array}{c} \textbf{0.0260} \\ \pm \textbf{0.0005} \end{array}$	$\begin{array}{c} \textbf{0.0233} \\ \pm \textbf{0.0004} \end{array}$	$\begin{array}{c} \textbf{0.0239} \\ \pm \textbf{0.0020} \end{array}$	$\begin{array}{c} \textbf{0.0419} \\ \pm \textbf{0.0011} \end{array}$
	Baseline	$\begin{array}{c} 1.1099 \\ \pm 0.0785 \end{array}$	$\substack{1.7452 \\ \pm 0.0467}$	$\begin{array}{c} 0.1248 \\ \scriptstyle{\pm 0.0137} \end{array}$	$\begin{array}{c} 0.6938 \\ \pm 0.2670 \end{array}$	$\substack{2.2074 \\ \pm 0.1852}$	$\begin{array}{c} 1.7684 \\ \scriptstyle{\pm 0.0941} \end{array}$	$0.9399 \\ \pm 0.0257$	$^{1.4118}_{\pm 0.0722}$
MAE^F_symm	. 0.1	0.1116	0.2262	0.0718 ± 0.0057	$0.0243 \\ \pm 0.0005$	$\begin{array}{c} 0.1979 \\ \scriptstyle{\pm 0.0024} \end{array}$	$\begin{array}{c} 0.1863 \\ \scriptstyle{\pm 0.0009} \end{array}$	$\begin{array}{c} 0.0418 \\ \scriptstyle{\pm 0.0046} \end{array}$	$0.0988 \\ \pm 0.0069$
ıvı∧∟symm	$\alpha = 0.1$	±0.0057	± 0.0107						
IVI△∟symm	$\alpha = 0.1$ $\alpha = 1.0$	$ \begin{array}{r} \pm 0.0057 \\ 0.0057 \\ \pm 0.0003 \end{array} $	0.0129 ±0.0004	0.0160 ±0.0005	$0.0066 \\ \pm 0.0014$	$0.0084 \\ \pm 0.0003$	$\begin{array}{c} 0.0083 \\ \pm 0.0002 \end{array}$	$\begin{array}{c} 0.0039 \\ \scriptstyle{\pm 0.0004} \end{array}$	$\begin{array}{c} 0.0076 \\ \pm 0.0002 \end{array}$
WI∏∟symm		0.0057	0.0129	0.0160					
WI∏∟symm	$\alpha = 1.0$	$0.0057 \\ \pm 0.0003 \\ \hline 0.0012$	$0.0129 \atop \pm 0.0004 \atop 0.0023$	$0.0160 \atop \pm 0.0005 \atop 0.0010$	±0.0014	±0.0003 0.0013	±0.0002 0.0018	±0.0004 0.0008	±0.0002 0.0016

A.9 Robustness to noise

In this subsection, we evaluate the performance of the ML models under the assumption that the position measurements are impacted by noise. To simulate measurement noise, we impose white noise on the particle positions at each time step. Then, we compute particle velocities and accelerations from the noisy positions. Here, we consider the following equation to impose noise on the measured positions:

$$\tilde{r}_{i\,k}^t \leftarrow r_{i\,k}^t + \beta \times X_{i\,k}^t \tag{21}$$

where $\tilde{r}_{i,k}^t$ is the k-th dimension of the noisy position of particle i at time t, $X_{i,k}^t \sim \mathcal{N}(0,1)$ is the random number sampled independently from the standard normal distribution and β is a constant controlling the level of noise. The second term in Eq. (21) represents the noise that is relevant to how we measure the position and how we discretize the space.

Different values for β will result in different noise levels for both inputs (position and velocity) and the learning target (acceleration). Here, we define the noise level as the **average relative change of the target**:

noise level =
$$\frac{1}{T} \frac{1}{|V|} \frac{1}{d} \sum_{t=1}^{T} \sum_{i \in V} \sum_{k \in d} \frac{|\tilde{a}_{i,k}^t - a_{i,k}^t|}{|a_{i,k}^t|}$$
 (22)

Here, $\tilde{a}_{i,k}^t$ is the k-th dimension of the noisy acceleration of particle i at time t^1 . We test 1e-7, 5e-7, 1e-6, 5e-6 and 1e-5 as the values for β . The corresponding noise levels of each dataset are summarized in Table 12.

	Spring dim=2	Spring dim=3	Charge dim=2	Charge dim=3	Orbital dim=2	Orbital dim=3	Discnt dim=2	Discnt dim=3
β =1e-7	0.0117	0.0075	0.3057	1.6369	0.0036	0.0092	0.0102	0.0187
β =5e-7	0.0405	0.0347	1.6401	6.1344	0.0182	0.0399	0.0515	0.0696
β =1e-6	0.1509	0.0790	3.0269	18.979	0.0369	0.0786	0.0979	0.1284
β =5e-6	0.5137	0.3936	14.767	43.030	0.1696	0.3980	0.4634	0.9941
β =1e-5	0.8897	0.7108	29.881	119.34	0.3664	0.8667	0.9809	1.9767

Table 12: The noise level (Eq. (22)) of each dataset with different values for β .

Table 13 and Table 14 report the performances of baseline and PIG'N'PI to learn pairwise force with the noisy input.

The results show the performance of PIG'N'PI decreases with increasing noise level. This makes sense because adding noise makes the training target less similar to the uncorrupted target that is associated with the pairwise force (note that we do not corrupt the ground-truth pairwise forces during evaluation). However, PIG'N'PI can still preform reasonably well with small scale noise.

The performance of baseline model fluctuates significantly with different noise levels. This also makes sense because the baseline model does not learn the particle interactions.

Developing PIG'N'PI further to make it even more robust to noisy input is left for future work.

¹When computing the noise level, we only consider those $|a_{i,k}^t|$ that are strictly larger than zero because we want to avoid dividing zero.

Table 13: Quality of pairwise force prediction of the baseline model with noisy data. The imposed noise corresponds to Eq. (21). "Uncorrupted" refers to the data without noise. Results averaged across five experiments.

-		Ci	Ci	Channa	Channa	O.I.:4-1	O-l-:4-1	D:	D:4
		Spring dim=2	Spring dim=3	dim=2	Charge dim=3	Orbital dim=2	Orbital dim=3	dim=2	Discnt dim=3
	Uncorrupted	$\begin{array}{c} 0.0565 \\ \pm 0.0023 \end{array}$	$\begin{array}{c} 0.1076 \\ \scriptstyle{\pm 0.0012} \end{array}$	$\begin{array}{c} 0.2521 \\ \pm 0.0173 \end{array}$	$\begin{array}{c} 0.3824 \\ \scriptstyle{\pm 0.0559} \end{array}$	$\begin{array}{c} 0.0437 \\ \scriptstyle{\pm 0.0026} \end{array}$	$\begin{array}{c} 0.0439 \\ \scriptstyle{\pm 0.0014} \end{array}$	$\begin{array}{c} 0.0592 \\ \scriptstyle{\pm 0.0015} \end{array}$	$\begin{array}{c} 0.1171 \\ \scriptstyle{\pm 0.0010} \end{array}$
MAE_{acc}	β =1e-7	0.0586 ±0.0016	$0.1085 \\ \pm 0.0023$	$\begin{array}{c} 0.2753 \\ \scriptstyle{\pm 0.0194} \end{array}$	$0.3544 \atop \pm 0.0220$	$\begin{array}{c} 0.0435 \\ \pm 0.0006 \end{array}$	$\begin{array}{c} 0.0446 \\ \pm 0.0009 \end{array}$	$0.0586 \atop \pm 0.0013$	$\begin{array}{c} 0.1158 \\ \pm 0.0034 \end{array}$
	β =5e-7	0.0639 ±0.0037	$\begin{array}{c} 0.1165 \\ \scriptstyle{\pm 0.0027} \end{array}$	$\begin{array}{c} 0.2735 \\ \scriptstyle{\pm 0.0246} \end{array}$	$\begin{array}{c} 0.4071 \\ \scriptstyle{\pm 0.0286} \end{array}$	$\begin{array}{c} 0.0497 \\ \scriptstyle{\pm 0.0014} \end{array}$	$\begin{array}{c} 0.0571 \\ \scriptstyle{\pm 0.0010} \end{array}$	$\begin{array}{c} 0.0719 \\ \scriptstyle{\pm 0.0028} \end{array}$	$\begin{array}{c} 0.1317 \\ \pm 0.0046 \end{array}$
	β =1e-6	$0.0767 \\ \pm 0.0012$	$\begin{array}{c} 0.1340 \\ \scriptstyle{\pm 0.0013} \end{array}$	$\begin{array}{c} 0.2933 \\ \scriptstyle{\pm 0.0159} \end{array}$	$\begin{array}{c} 0.3973 \\ \scriptstyle{\pm 0.0391} \end{array}$	$\begin{array}{c} 0.0654 \\ \scriptstyle{\pm 0.0006} \end{array}$	$\begin{array}{c} 0.0828 \\ \scriptstyle{\pm 0.0008} \end{array}$	$\begin{array}{c} 0.0890 \\ \scriptstyle{\pm 0.0013} \end{array}$	$\begin{array}{c} 0.1556 \\ \pm 0.0031 \end{array}$
	β =5e-6	$\begin{array}{c} 0.2430 \\ \scriptstyle{\pm 0.0011} \end{array}$	$\begin{array}{c} 0.3758 \\ \scriptstyle{\pm 0.0016} \end{array}$	$\underset{\pm 0.0198}{0.4138}$	$\begin{array}{c} 0.6577 \\ \scriptstyle{\pm 0.0276} \end{array}$	$\begin{array}{c} 0.2228 \\ \scriptstyle{\pm 0.0014} \end{array}$	$\begin{array}{c} 0.3331 \\ \scriptstyle{\pm 0.0013} \end{array}$	$\begin{array}{c} 0.2553 \\ \scriptstyle{\pm 0.0032} \end{array}$	$0.4174 \\ \pm 0.0016$
	β =1e-5	$\begin{array}{c} 0.4694 \\ \scriptstyle{\pm 0.0039} \end{array}$	$\begin{array}{c} 0.7196 \\ \scriptstyle{\pm 0.0021} \end{array}$	$\underset{\pm 0.0159}{0.6222}$	$\substack{1.0038 \\ \pm 0.0572}$	$\begin{array}{c} 0.4370 \\ \scriptstyle{\pm 0.0011} \end{array}$	$\begin{array}{c} 0.6683 \\ \pm 0.0020 \end{array}$	$\begin{array}{c} 0.4809 \\ \pm 0.0020 \end{array}$	$\begin{array}{c} 0.7552 \\ \pm 0.0040 \end{array}$
	Uncorrupted	$\substack{2.3979 \\ \pm 0.2095}$	$\begin{array}{c} 3.8952 \\ \scriptstyle{\pm 0.7178} \end{array}$	$\begin{array}{c} 1.1832 \\ \scriptstyle{\pm 0.0955} \end{array}$	$\begin{array}{c} 0.6447 \\ \scriptstyle{\pm 0.1118} \end{array}$	$\begin{array}{c} 4.1010 \\ \scriptstyle{\pm 0.1467} \end{array}$	$\begin{array}{c} 3.5379 \\ \scriptstyle{\pm 0.7571} \end{array}$	$\substack{1.6536 \\ \pm 0.0640}$	$^{2.5803}_{\pm 0.2886}$
MAE_{ef}	β =1e-7	$^{1.9321}_{\pm 0.6308}$	$\begin{array}{c} 4.2515 \\ \scriptstyle{\pm 0.4175} \end{array}$	$^{1.3544}_{\pm 0.0752}$	$\begin{array}{c} 0.5249 \\ \scriptstyle{\pm 0.0468} \end{array}$	$\begin{array}{c} 3.3631 \\ \scriptstyle{\pm 0.7493} \end{array}$	$\begin{array}{c} 3.8075 \\ \pm 0.1573 \end{array}$	$\substack{1.6651 \\ \pm 0.2816}$	$^{2.6424}_{\pm 0.2322}$
	β =5e-7	$\substack{2.5900 \\ \pm 0.4020}$	$\begin{array}{c} 4.0157 \\ \scriptstyle{\pm 0.3880} \end{array}$	$\substack{1.2892 \\ \pm 0.0139}$	$\begin{array}{c} 0.6376 \\ \scriptstyle{\pm 0.0887} \end{array}$	$\substack{2.5351 \\ \pm 0.8932}$	$\begin{array}{c} 3.5454 \\ \pm 0.4215 \end{array}$	$\substack{1.6866 \\ \pm 0.1694}$	$\begin{array}{c} 1.9837 \\ \pm 0.2123 \end{array}$
	β =1e-6	$\substack{2.6234 \\ \pm 0.9036}$	$\begin{array}{c} 3.8559 \\ \pm 0.4356 \end{array}$	$\substack{1.3248 \\ \pm 0.0811}$	$\begin{array}{c} 0.5286 \\ \scriptstyle{\pm 0.0782} \end{array}$	$\begin{array}{c} 4.0880 \\ \pm 1.3048 \end{array}$	$\begin{array}{c} 3.7811 \\ \pm 0.3673 \end{array}$	$^{1.3008}_{\pm 0.2183}$	$\begin{array}{c} 2.3136 \\ \scriptstyle{\pm 0.4424} \end{array}$
	β =5e-6	1.6493 ±0.8436	$\begin{array}{c} 3.9151 \\ \pm 0.5906 \end{array}$	$^{1.3440}_{\pm 0.1431}$	$\begin{array}{c} 0.6125 \\ \scriptstyle{\pm 0.0889} \end{array}$	$\begin{array}{c} 3.9054 \\ \scriptstyle{\pm 1.4067} \end{array}$	$\begin{array}{c} 3.2323 \\ \scriptstyle{\pm 0.6269} \end{array}$	$1.3307 \\ \pm 0.1672$	$\substack{2.0825 \\ \pm 0.3995}$
	β =1e-5	$\substack{2.2223 \\ \pm 0.4609}$	$\begin{array}{c} 3.3053 \\ \scriptstyle{\pm 0.4277} \end{array}$	$\substack{1.2780 \\ \pm 0.1208}$	$\begin{array}{c} 0.6939 \\ \scriptstyle{\pm 0.1686} \end{array}$	$\substack{4.4303 \\ \pm 0.9807}$	$\underset{\pm 0.5783}{2.9186}$	$1.2169 \atop \pm 0.3209$	$^{1.9050}_{\pm 0.3288}$
	Uncorrupted	$\begin{array}{c} 11.652 \\ \scriptstyle{\pm 0.9890} \end{array}$	$\begin{array}{c} 20.967 \\ \pm 3.8552 \end{array}$	$\begin{array}{c} 6.8310 \\ \scriptstyle{\pm 0.5548} \end{array}$	$\begin{array}{c} 3.8038 \\ \pm 0.7523 \end{array}$	$18.194 \atop \pm 0.6884$	$^{16.677}_{\pm 3.5212}$	$10.786 \atop \pm 0.3764$	$15.651 \atop \pm 1.7983$
MAE_{nf}	β =1e-7	9.3805 ±3.0398	$\begin{array}{c} 22.903 \\ \pm 2.3024 \end{array}$	$7.8383 \atop \pm 0.4344$	$\begin{array}{c} 3.0275 \\ \scriptstyle{\pm 0.2899} \end{array}$	$^{14.940}_{\pm 3.3092}$	$\begin{array}{c} 17.918 \\ \scriptstyle{\pm 0.7365} \end{array}$	$\begin{array}{c} 10.838 \\ \scriptstyle{\pm 1.8261} \end{array}$	$15.971 \\ \scriptstyle{\pm 1.4671}$
	β =5e-7	12.588 ±1.9510	$\underset{\pm 2.0799}{21.635}$	$\begin{array}{c} 7.455 \\ \scriptstyle{\pm 0.0881} \end{array}$	$\begin{array}{c} 3.751 \\ \scriptstyle{\pm 0.5713} \end{array}$	$11.284 \atop \pm 3.9460$	$\substack{16.671 \\ \pm 1.9563}$	$10.957 \atop \scriptstyle{\pm 1.0616}$	11.936 ±1.3494
	β =1e-6	$12.746 \atop \pm 4.3777$	$\begin{array}{c} 20.718 \\ \scriptstyle{\pm 2.3664} \end{array}$	$\begin{array}{c} 7.661 \\ \scriptstyle{\pm 0.4736} \end{array}$	$\substack{2.987 \\ \pm 0.5201}$	$18.104 \newline \pm 5.7265$	$17.759 \\ \scriptstyle{\pm 1.7564}$	$\begin{array}{c} 8.3936 \\ \pm 1.4703 \end{array}$	$14.016 \\ \pm 2.7942$
	β =5e-6	$7.9912 \\ \pm 4.0598$	$^{21.037}_{\pm 3.1630}$	$\begin{array}{c} 7.8270 \\ \scriptstyle{\pm 0.8340} \end{array}$	$\begin{array}{c} 3.6208 \\ \scriptstyle{\pm 0.5847} \end{array}$	$17.303 \atop \scriptstyle{\pm 6.1886}$	$15.218 \\ \pm 2.9087$	$\begin{array}{c} 8.4946 \\ \pm 1.0542 \end{array}$	$12.392 \\ \pm 2.4643$
	β=1e-5	$10.798 \\ \pm 2.2379$	$17.752 \\ \pm 2.3123$	$7.5451 \atop \pm 0.7052$	$\begin{array}{c} 4.2474 \\ \pm 1.0325 \end{array}$	$19.595 \\ \pm 4.3285$	$13.720 \\ \pm 2.6955$	$\begin{array}{c} 7.6793 \\ \pm 2.0393 \end{array}$	$11.189 \\ \pm 2.0076$
	Uncorrupted	$1.1099 \\ \pm 0.0785$	$\begin{array}{c} 1.7452 \\ \pm 0.0467 \end{array}$	$\begin{array}{c} 0.1248 \\ \scriptstyle{\pm 0.0137} \end{array}$	$\begin{array}{c} 0.6938 \\ \pm 0.2670 \end{array}$	$\substack{2.2074 \\ \pm 0.1852}$	$\substack{1.7684 \\ \pm 0.0941}$	$0.9399 \atop \pm 0.0257$	$^{1.4118}_{\pm 0.0722}$
MAE^F_{symm}	β =1e-7	$\begin{array}{c} 1.0733 \\ \pm 0.1043 \end{array}$	$\substack{1.8067 \\ \pm 0.0760}$	$\begin{array}{c} 0.1232 \\ \pm 0.0352 \end{array}$	$\begin{array}{c} 0.4565 \\ \pm 0.0538 \end{array}$	$\substack{1.9961 \\ \pm 0.1710}$	$\begin{array}{c} 1.9239 \\ \pm 0.1455 \end{array}$	$\substack{1.0063 \\ \pm 0.1074}$	$^{1.4453}_{\pm 0.0999}$
- ,	β =5e-7	$\begin{array}{c} 0.9284 \\ \pm 0.0798 \end{array}$	$^{1.8013}_{\pm 0.0401}$	$\begin{array}{c} 0.1666 \\ \scriptstyle{\pm 0.0190} \end{array}$	$\begin{array}{c} 0.6596 \\ \scriptstyle{\pm 0.1836} \end{array}$	$\substack{2.0250 \\ \pm 0.1278}$	$\substack{1.7911 \\ \pm 0.0679}$	$\begin{array}{c} 0.9921 \\ \scriptstyle{\pm 0.1084} \end{array}$	$^{1.3530}_{\pm 0.0336}$
	β =1e-6	1.0539 ±0.0690	$\substack{1.6816 \\ \pm 0.0809}$	$\begin{array}{c} 0.1592 \\ \pm 0.0224 \end{array}$	$\begin{array}{c} 0.3622 \\ \scriptstyle{\pm 0.2052} \end{array}$	$\substack{2.1475 \\ \pm 0.1492}$	$^{1.7512}_{\pm 0.1160}$	$0.9143 \\ \pm 0.1050$	1.3089 ±0.1026
	β =5e-6	$\begin{array}{c} 0.8486 \\ \scriptstyle{\pm 0.0614} \end{array}$	$^{1.6024}_{\pm 0.0432}$	$\begin{array}{c} 0.1551 \\ \scriptstyle{\pm 0.0126} \end{array}$	$\begin{array}{c} 0.5979 \\ \scriptstyle{\pm 0.2170} \end{array}$	$^{1.9721}_{\pm 0.1302}$	$\begin{array}{c} 1.7956 \\ \pm 0.0726 \end{array}$	$\begin{array}{c} 0.8552 \\ \pm 0.1154 \end{array}$	$\begin{array}{c} 1.1735 \\ \pm 0.1105 \end{array}$
	β =1e-5	0.7940 ±0.1133	$^{1.4555}_{\pm 0.0619}$	$\begin{array}{c} 0.1581 \\ \scriptstyle{\pm 0.0241} \end{array}$	$\begin{array}{c} 0.7711 \\ \scriptstyle{\pm 0.3974} \end{array}$	$\underset{\pm 0.1608}{2.0862}$	$\begin{array}{c} 1.5985 \\ \pm 0.0812 \end{array}$	$\begin{array}{c} 0.7857 \\ \scriptstyle{\pm 0.1024} \end{array}$	$^{1.1565}_{\pm 0.0908}$

Table 14: Quality of pairwise force prediction of the PIG'N'PI with noisy data. The imposed noise corresponds to Eq. (21). "Uncorrupted" refers to the data without noise. Results averaged across five experiments.

		Spring dim=2	Spring dim=3	Charge dim=2	Charge dim=3	Orbital dim=2	Orbital dim=3	Discnt dim=2	Discnt dim=3
	Uncorrupted	$0.0206 \atop \pm 0.0009$	$\begin{array}{c} 0.0278 \\ \scriptstyle{\pm 0.0021} \end{array}$	$0.0425 \\ \pm 0.0053$	$\begin{array}{c} 0.1191 \\ \pm 0.0027 \end{array}$	$\begin{array}{c} 0.0202 \\ \scriptstyle \pm 0.0003 \end{array}$	$\begin{array}{c} 0.0182 \\ \scriptstyle{\pm 0.0003} \end{array}$	$\begin{array}{c} 0.0227 \\ \scriptstyle{\pm 0.0019} \end{array}$	$0.0399 \atop \pm 0.0011$
MAE_{acc}	β =1e-7	$\begin{array}{c} 0.0213 \\ \scriptstyle{\pm 0.0009} \end{array}$	$\begin{array}{c} 0.0305 \\ \scriptstyle{\pm 0.0020} \end{array}$	$\begin{array}{c} 0.0421 \\ \scriptstyle{\pm 0.0031} \end{array}$	$\begin{array}{c} 0.1208 \\ \scriptstyle{\pm 0.0030} \end{array}$	$\begin{array}{c} 0.0208 \\ \scriptstyle{\pm 0.0005} \end{array}$	$\begin{array}{c} 0.0203 \\ \scriptstyle{\pm 0.0005} \end{array}$	$\begin{array}{c} 0.0274 \\ \scriptstyle{\pm 0.0045} \end{array}$	$\begin{array}{c} 0.0429 \\ \pm 0.0009 \end{array}$
	β =5e-7	0.0315 ±0.0007	0.0449 ±0.0012	$0.0510 \\ \pm 0.0020$	0.1393 ±0.0055	0.0302 ±0.0004	0.0374 ±0.0003	$0.0377 \\ \pm 0.0008$	$0.0614 \\ \pm 0.0006$
	β =1e-6	0.0499 ±0.0004	0.0720 ±0.0007	0.0697 ±0.0021	0.1704 ±0.0038	0.0473 ±0.0005	0.0658 ±0.0001	0.0585 ±0.0038	0.0902 ±0.0012
	β =5e-6	0.2050 ±0.0004	0.3062 ±0.0004	0.2209 ±0.0032	0.4163 ±0.0063	0.2033 ±0.0003	$0.3088 \\ \pm 0.0010$	0.2124 ±0.0027	0.3257 ±0.0006
	β =1e-5	0.4060 ±0.0009	0.6136 ±0.0008	0.4215 ±0.0016	$0.7661 \\ \pm 0.0097$	0.4102 ±0.0009	$0.6348 \atop \pm 0.0026$	0.4146 ±0.0017	0.6231 ±0.0007
	Uncorrupted	$\begin{array}{c} 0.0063 \\ \pm 0.0002 \end{array}$	$\begin{array}{c} 0.0101 \\ \pm 0.0007 \end{array}$	$0.0136 \atop \pm 0.0023$	$\begin{array}{c} 0.0363 \\ \scriptstyle{\pm 0.0015} \end{array}$	$0.0093 \\ \scriptstyle{\pm 0.0002}$	$\begin{array}{c} 0.0095 \\ \scriptstyle{\pm 0.0001} \end{array}$	$\begin{array}{c} 0.0040 \\ \scriptstyle{\pm 0.0004} \end{array}$	$0.0079 \\ \pm 0.0002$
MAE_{ef}	β =1e-7	0.0064 ±0.0002	$\begin{array}{c} 0.0107 \\ \pm 0.0007 \end{array}$	$0.0135 \atop \pm 0.0016$	$\begin{array}{c} 0.0359 \\ \scriptstyle{\pm 0.0009} \end{array}$	$0.0092 \atop \pm 0.0003$	$0.0101 \\ \pm 0.0003$	$0.0047 \\ \scriptstyle{\pm 0.0010}$	0.0082 ±0.0001
	β =5e-7	$0.0068 \\ \pm 0.0002$	$\begin{array}{c} 0.0112 \\ \scriptstyle{\pm 0.0005} \end{array}$	$\begin{array}{c} 0.0143 \\ \scriptstyle{\pm 0.0011} \end{array}$	$\begin{array}{c} 0.0381 \\ \scriptstyle{\pm 0.0016} \end{array}$	$\begin{array}{c} 0.0097 \\ \scriptstyle{\pm 0.0001} \end{array}$	$\begin{array}{c} 0.0111 \\ \scriptstyle{\pm 0.0001} \end{array}$	$\begin{array}{c} 0.0043 \\ \pm 0.0002 \end{array}$	$0.0089 \\ \pm 0.0001$
	β =1e-6	0.0078 ±0.0001	$\begin{array}{c} 0.0131 \\ \scriptstyle{\pm 0.0004} \end{array}$	$\begin{array}{c} 0.0163 \\ \scriptstyle{\pm 0.0013} \end{array}$	$\begin{array}{c} 0.0413 \\ \scriptstyle{\pm 0.0016} \end{array}$	$\begin{array}{c} 0.0108 \\ \pm 0.0002 \end{array}$	$\begin{array}{c} 0.0136 \\ \scriptstyle{\pm 0.0002} \end{array}$	$0.0055 \\ \pm 0.0013$	$0.0106 \\ \pm 0.0003$
	β =5e-6	$0.0162 \\ \pm 0.0002$	$\begin{array}{c} 0.0275 \\ \scriptstyle{\pm 0.0004} \end{array}$	$\begin{array}{c} 0.0265 \\ \pm 0.0024 \end{array}$	$\begin{array}{c} 0.0572 \\ \pm 0.0024 \end{array}$	$\begin{array}{c} 0.0223 \\ \scriptstyle{\pm 0.0005} \end{array}$	$0.0373 \atop \pm 0.0010$	$\begin{array}{c} 0.0114 \\ \scriptstyle{\pm 0.0027} \end{array}$	$0.0211 \\ \pm 0.0006$
	β =1e-5	0.0321 ±0.0007	$\begin{array}{c} 0.0545 \\ \pm 0.0006 \end{array}$	$\begin{array}{c} 0.0411 \\ \scriptstyle{\pm 0.0005} \end{array}$	$\begin{array}{c} 0.0984 \\ \scriptstyle{\pm 0.0065} \end{array}$	$\begin{array}{c} 0.0421 \\ \scriptstyle{\pm 0.0004} \end{array}$	$\begin{array}{c} 0.0826 \\ \scriptstyle{\pm 0.0029} \end{array}$	$0.0247 \\ \pm 0.0031$	0.0410 ±0.0007
	Uncorrupted	$0.0219 \atop \pm 0.0010$	$\begin{array}{c} 0.0292 \\ \pm 0.0022 \end{array}$	$\begin{array}{c} 0.0488 \\ \pm 0.0059 \end{array}$	$\begin{array}{c} 0.1317 \\ \scriptstyle{\pm 0.0033} \end{array}$	$\begin{array}{c} 0.0260 \\ \scriptstyle{\pm 0.0005} \end{array}$	$\begin{array}{c} 0.0233 \\ \scriptstyle{\pm 0.0004} \end{array}$	$\begin{array}{c} 0.0239 \\ \scriptstyle{\pm 0.0020} \end{array}$	$0.0419 \atop \pm 0.0011$
MAE_{nf}	β =1e-7	$0.0230 \atop \pm 0.0010$	$\begin{array}{c} 0.0324 \\ \scriptstyle{\pm 0.0021} \end{array}$	$\begin{array}{c} 0.0486 \\ \pm 0.0035 \end{array}$	$\begin{array}{c} 0.1334 \\ \scriptstyle{\pm 0.0034} \end{array}$	$\begin{array}{c} 0.0266 \\ \pm 0.0007 \end{array}$	$\begin{array}{c} 0.0260 \\ \scriptstyle{\pm 0.0006} \end{array}$	$\begin{array}{c} 0.0294 \\ \scriptstyle \pm 0.0046 \end{array}$	$\begin{array}{c} 0.0456 \\ \pm 0.0008 \end{array}$
	β =5e-7	$0.0370 \atop \pm 0.0007$	$\begin{array}{c} 0.0528 \\ \scriptstyle{\pm 0.0011} \end{array}$	$\begin{array}{c} 0.0607 \\ \scriptstyle{\pm 0.0024} \end{array}$	$\begin{array}{c} 0.1581 \\ \scriptstyle{\pm 0.0058} \end{array}$	$\begin{array}{c} 0.0386 \\ \pm 0.0005 \end{array}$	$\begin{array}{c} 0.0481 \\ \pm 0.0004 \end{array}$	$\begin{array}{c} 0.0439 \\ \scriptstyle{\pm 0.0008} \end{array}$	$\begin{array}{c} 0.0704 \\ \scriptstyle{\pm 0.0007} \end{array}$
	β =1e-6	$\begin{array}{c} 0.0610 \\ \scriptstyle{\pm 0.0004} \end{array}$	$\begin{array}{c} 0.0880 \\ \scriptstyle{\pm 0.0007} \end{array}$	$\begin{array}{c} 0.0846 \\ \scriptstyle{\pm 0.0023} \end{array}$	$\begin{array}{c} 0.1974 \\ \scriptstyle{\pm 0.0046} \end{array}$	$\begin{array}{c} 0.0606 \\ \scriptstyle{\pm 0.0007} \end{array}$	$\begin{array}{c} 0.0846 \\ \scriptstyle{\pm 0.0002} \end{array}$	$\begin{array}{c} 0.0701 \\ \pm 0.0038 \end{array}$	$\begin{array}{c} 0.1070 \\ \scriptstyle{\pm 0.0011} \end{array}$
	β =5e-6	$\begin{array}{c} 0.2605 \\ \scriptstyle{\pm 0.0003} \end{array}$	$\begin{array}{c} 0.3876 \\ \scriptstyle{\pm 0.0004} \end{array}$	$\begin{array}{c} 0.2782 \\ \scriptstyle{\pm 0.0036} \end{array}$	$\begin{array}{c} 0.5092 \\ \scriptstyle{\pm 0.0082} \end{array}$	$\begin{array}{c} 0.2602 \\ \pm 0.0006 \end{array}$	$\begin{array}{c} 0.3968 \\ \pm 0.0011 \end{array}$	$\begin{array}{c} 0.2673 \\ \pm 0.0027 \end{array}$	$\begin{array}{c} 0.4078 \\ \scriptstyle{\pm 0.0005} \end{array}$
	β =1e-5	$\begin{array}{c} 0.5143 \\ \scriptstyle{\pm 0.0008} \end{array}$	$\begin{array}{c} 0.7800 \\ \scriptstyle{\pm 0.0008} \end{array}$	$\begin{array}{c} 0.5353 \\ \scriptstyle{\pm 0.0019} \end{array}$	$\begin{array}{c} 0.9458 \\ \scriptstyle{\pm 0.0102} \end{array}$	$\begin{array}{c} 0.5273 \\ \scriptstyle{\pm 0.0009} \end{array}$	$\begin{array}{c} 0.8101 \\ \pm 0.0029 \end{array}$	$\begin{array}{c} 0.5250 \\ \pm 0.0019 \end{array}$	$\begin{array}{c} 0.7843 \\ \scriptstyle{\pm 0.0006} \end{array}$
	Uncorrupted	$0.0075 \\ \pm 0.0003$	$\begin{array}{c} 0.0133 \\ \scriptstyle{\pm 0.0008} \end{array}$	$\begin{array}{c} 0.0185 \\ \pm 0.0036 \end{array}$	$\begin{array}{c} 0.0345 \\ \pm 0.0017 \end{array}$	$\begin{array}{c} 0.0136 \\ \scriptstyle{\pm 0.0004} \end{array}$	$\begin{array}{c} 0.0134 \\ \scriptstyle{\pm 0.0004} \end{array}$	$\begin{array}{c} 0.0026 \\ \scriptstyle{\pm 0.0004} \end{array}$	$\begin{array}{c} 0.0066 \\ \pm 0.0001 \end{array}$
MAE^F_{symm}	β =1e-7	$\begin{array}{c} 0.0076 \\ \scriptstyle{\pm 0.0002} \end{array}$	$\begin{array}{c} 0.0139 \\ \scriptstyle{\pm 0.0008} \end{array}$	$\begin{array}{c} 0.0180 \\ \scriptstyle{\pm 0.0030} \end{array}$	$\begin{array}{c} 0.0339 \\ \scriptstyle{\pm 0.0010} \end{array}$	$\begin{array}{c} 0.0132 \\ \scriptstyle{\pm 0.0005} \end{array}$	$\begin{array}{c} 0.0141 \\ \scriptstyle{\pm 0.0005} \end{array}$	$\begin{array}{c} 0.0031 \\ \scriptstyle{\pm 0.0006} \end{array}$	$0.0069 \\ \pm 0.0000$
	β =5e-7	0.0083 ±0.0003	$0.0149 \atop \pm 0.0007$	$\begin{array}{c} 0.0201 \\ \pm 0.0022 \end{array}$	$\begin{array}{c} 0.0369 \\ \scriptstyle{\pm 0.0016} \end{array}$	$0.0139 \atop \pm 0.0002$	$0.0155 \\ \pm 0.0002$	$0.0032 \atop \pm 0.0002$	$0.0079 \\ \pm 0.0002$
	β =1e-6	$\begin{array}{c} 0.0098 \\ \scriptstyle{\pm 0.0001} \end{array}$	$\begin{array}{c} 0.0173 \\ \scriptstyle{\pm 0.0005} \end{array}$	$\begin{array}{c} 0.0223 \\ \scriptstyle{\pm 0.0017} \end{array}$	$\begin{array}{c} 0.0407 \\ \pm 0.0012 \end{array}$	$0.0154 \atop \pm 0.0002$	$0.0194 \atop \pm 0.0005$	$0.0046 \atop \pm 0.0012$	$0.0096 \atop \pm 0.0001$
	β =5e-6	0.0222 ±0.0003	$0.0382 \atop \pm 0.0004$	$0.0354 \\ \pm 0.0023$	$0.0653 \\ \pm 0.0023$	$0.0314 \atop \pm 0.0008$	$0.0529 \atop \pm 0.0014$	$0.0124 \atop \pm 0.0037$	$0.0238 \atop \pm 0.0011$
	β =1e-5	$0.0450 \\ \pm 0.0010$	$\begin{array}{c} 0.0768 \\ \scriptstyle{\pm 0.0011} \end{array}$	$\begin{array}{c} 0.0485 \\ \pm 0.0016 \end{array}$	$\begin{array}{c} 0.1184 \\ \scriptstyle{\pm 0.0085} \end{array}$	$\underset{\pm 0.0008}{0.0601}$	$\begin{array}{c} 0.1174 \\ \scriptstyle{\pm 0.0049} \end{array}$	$\begin{array}{c} 0.0314 \\ \scriptstyle{\pm 0.0048} \end{array}$	$\begin{array}{c} 0.0518 \\ \pm 0.0011 \end{array}$

A.10 Visualization of force and potential functions used in simulation

Fig. 11 shows the inter-particle potential energy P and the inter-particle pairwise force F used for generating the simulations. P and F are the functions of relative distance.

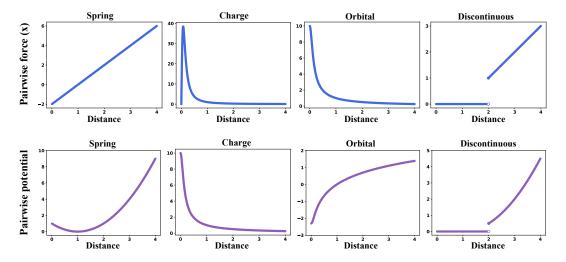


Figure 11: Visualization of pairwise force and potential with different distances. Blue color shows the pairwise force in x dimension as the function of the relative distance between particles. Purple color in second row shows the pairwise potential with different distance. In this visualization, we set the electric charge and particle masses to one.